# Volatile element depletion of the Moon – the roles of pre-cursors, post-impact disk dynamics, and core formation.

K. Righter, Mailcode XI2, NASA-JSC, 2101 NASA Parkway, Houston, TX 77058; kevin.righter-1@nasa.gov.

The compositional and isotopic similarity of Earth's primitive upper mantle (PUM) and the Moon has bolstered the idea that the Moon was derived from the proto-Earth, but the Moon's inventory of volatile lithophile elements – Na, K, Rb and Cs – are lower than in Earth's PUM by a factor of 4 to 5. The abundances of fourteen other volatile elements exhibit siderophile behavior (volatile siderophile elements or VSE; P, As, Cu, Ag, Sb, Ga, Ge, Bi, Pb, Zn, Sn, Cd, In, and Tl) that could be used to evaluate whether the Moon was derived from the proto-Earth, and whether their depletion can be attributed to volatility or core formation. In this study, newly available core-mantle partitioning data are used, together with bulk Moon compositions, protolunar disk dynamics modelling to test the hypothesis that the Moon was derived from PUM-like material. At lunar core formation conditions, As, Sb, Ag, Ge, Bi, Sn are siderophile, whereas P, Cu, Ga, Pb, Zn, Cd, In and Tl are all weakly siderophile or lithophile. Most of the VSE can be explained by a combination of known processes – pre-cursor volatile depletion, melt-gas dynamics and equilibria in the protolunar disk, and core formation. Explaining this whole group of volatile elements may require a combination of mixing and separation of the newly formed Moon from remnant gas rich in the highest volatility VSEs. This large group of volatile elements informs a wide temperature range and offers a powerful test of melt-gas segregation mechanisms in the protolunar disk and lunar formation hypotheses.

**Introduction:** The similarity of Earth and Moon isotopic composition (O, Ti, Ca, Fe, Mg, etc.) coupled with physical aspects such as angular momentum, lunar mass, and inclination, have led to various impact models for the origin of the Moon. The canonical late impactor (1) model showed that an impactor:proto-Earth mass ratio of 1:9, with a relatively low impact velocity would result in an Earth-Moon system that has many of the observed properties of our own. With relaxation of angular momentum constraints, more energetic collisions such as in highly spun up impactor and proto-Earth (2,3) or 1:1 impactor:protoEarth scenarios (3,4) can also produce an Earth-Moon system as long as they are coupled with an angular momentum loss mechanism. Multiple smaller mass and energy impacts (5) can also produce an Earth-Moon system, with the overall energetics more similar to a canonical model. The latter three models are relatively new and grew out of the last decade of research exploring the details of angular momentum, lunar source material, and pre-impact spin state constraints, and have led to multiple working hypotheses for lunar origin (1-5).

The volatile element depletions in the Moon have been recognized for decades (6,7). Volatile elements can be depleted in the pre-cursor (or building blocks) of the Moon, they can be depleted during the impact and post-impact processes that formed the Moon, and then some can be partitioned into the Moon's metallic core. Although multiple explanations have been debated, and arguments have become more quantitative, the depletion of many volatile elements remains unexplained in detail. In this study, newly available core-mantle partitioning data for 14 volatile siderophile elements (VSE) (e.g., 8-12 and references therein) are used to evaluate the roles of pre-cursor volatility, disk dynamics, and core formation in establishing the lunar VSE depletion and test the hypothesis that the Moon was derived from PUM-like material. Examination of all 14 elements - P, As, Cu, Ag, Sb, Ga, Ge, Bi, Pb, Zn, Sn, Cd, In, and Tl – at once allows recognition of general trends among the volatile siderophile elements, without undue focus on one element.

The VSE content of the lunar mantle will be updated using published data from lunar samples (Apollo and Luna basalt and glass samples). The three processes that determine whether PUM-like material could make the Moon (pre-cursor volatile element depletion, proto-lunar disk dynamics, and lunar core formation) have been modelled to occur in 3 stages to separately asses their control on the VSE contents.

**Lunar mantle concentrations of VSE - constraints from samples:** Mantle concentrations are defined by correlations between the VSE and a refractory lithophile element (RLE) of comparable behavior during mantle melting (i.e., compatible or incompatible) in basalt and volcanic glass suites from differentiated bodies (13). Many lunar mantle melts (basalts and volcanic glasses) from the Apollo and lunar meteorite collections have been analyzed and are used to reconstruct the mantle source concentrations of the VSE using known and comparable behavior of the VSE and RLE, which are unfractionated during melting and differentiation [e.g., (14-19)] (see **Supplementary information Part 1, Figures S1 and S2 for summary and Extended Supplementary Table for full sample analyses and details**).

## Modelling the VSE content of the lunar mantle

In modelling the VSE content of the lunar mantle, several stages are considered which reflect known processes that contributed to the formation of the Moon: stage 1 represents the degree to which the bulk Moon composition was volatile depleted. Stage 2 represents the process(es) after the Moon-forming impact(s) that controlled the accretion of the Moon from a gas-melt disk. Stage 3 represents the syn- or post-accretion segregation of a metallic core and its equilibration with the mantle. These processes were likely separated in time and represent distinct processes and thus are referred to here as stages (Figure 1).

*Stage 1: Volatile depleted building blocks*

Most inner solar system bodies have a recognized volatile element depletion relative to chondritic proportions that originated with the building blocks or pre-cursors, and the Earth is no exception. Three different lunar bulk compositions that represent possible scenarios for Moon formation are considered: (A) bulk Moon is from the terrestrial primitive upper mantle (20-23) as suggested in some formation models for the Moon, (B) bulk Moon is from a Mars-sized (but initially more volatile-rich than PUM) impactor mantle for which we will use Mars as a proxy; the mantle and bulk composition of Mars are relatively well known from meteorite studies and geochemical constraints (24,25), and (C) bulk Moon is from a Mars-sized (but initially more volatile depleted than PUM) impactor mantle, similar in overall bulk composition to Earth. Bulk compositions are described in more detail and discussed in the **Supplementary information, part 2**.

*Stage 2: Proto-lunar disk dynamics*

Most lunar formation models predict that after an impact the Moon will accrete from a disk of material that surrounds the proto-Earth. This material is likely to be (or become upon cooling) a mixture of melt and gas, and so the volatile content of the Moon may depend on mixing within the disk (26) or partitioning between melt and gas (3), and the possibility of subsequent gas-melt segregation in the disk. Is there a gas-melt segregation mechanism that is consistent with the early lunar disk thermal structure that can also explain the pattern of volatile element depletion in the Moon?

Mixing between the inner volatile-depleted and outer volatile-bearing disk was proposed (26) as a way to explain the volatile depletions in the Moon, and is modelled here by modifying the bulk composition of the Moon to match the volatile lithophile element (Li, Na, K, Rb and Cs) concentrations in the lunar mantle, assuming they are due to mixing. Depletion of the volatile lithophile elements in the 3 bulk compositions is guided by comparisons with Earth's primitive upper mantle, where Moon/Earth ratios are known to be ~1 for Li, and ~0.25 for Na, K, Rb and Cs, and corresponding adjustments to volatile siderophile element contents must be made (**see Supplementary information part 3; Figure S3**).

Disk modelling has identified segregation mechanisms for melt and gas in the protolunar disk, but there is currently little agreement and a need for additional work. The details and timing of the early stages of lunar history are uncertain, but there are several physical settings and models that can segregate melt and gas, moving gas either inward or outward relative to the melt, including disk resonances, disk-Moon tidal interactions, or turbulence at the melt-gas interface (see discussion below). Gas-melt partitioning is captured with a simple term in equation 2 that quantifies the partitioning of an element between gas and silicate melt, and the gas fraction of the system, understanding that the specific mechanism has not yet been identified, as discussed below. This term is meant to be illustrative of possible gas-melt equilibrium and not demonstrative, but is motivated by expected behavior for these elements.

*Stage 3: Core formation*

Previous work has shown that a wide range of mantle siderophile element concentrations (e.g., Ni, Co, Mo, W, V, Cr) can be explained by the equilibration of a small metallic core with the mantle, at ~4.5 GPa, ~2273 K, and oxygen fugacity near IW-1 (27-29).

Metal/silicate partitioning can be predicted for 13 of the volatile siderophile elements using an expression which has been derived elsewhere [e.g., 30]:

$$\ln D(i) = a\ln fO_2 + b/T + cP/T + \ln\gamma_i + g[nbo/t] + h \qquad (1)$$

where $\gamma_i$ is the activity of element i in Fe metallic liquid (Table S1), nbo/t is the ratio of non-bridging oxygens to tetrahedrally coordinated cations and is a gauge of silicate melt compositional variation (a value of 2.8 for the bulk silicate Moon – [27]), and the coefficients a, b, c, g, and h are derived by multiple linear regression of various datasets. Regression coefficients and $\gamma_i$ for the VSE are available from recent experimental and partitioning studies (**Supplementary information; Table S1**). Thallium partitioning studies between metal, sulfide and silicate melt reveal that Tl is compatible in sulfur-rich or sulfide liquids, but weakly siderophile to lithophile at the S-poor conditions of lunar core formation, so we have adopted D(Tl) metal/silicate = 1 for the Moon (**Supplementary information; Table S1**). These new constraints can be applied to lunar core formation, with the additional assumption that equilibration between core metal and the lunar mantle is complete, which is the expected outcome in lunar-sized bodies experiencing impacts (31).

### Calculation of lunar mantle VSE resulting from 3 processes:

Combining these three stages can be done using a simple approach tracking gas, melt, and metallic liquid phases that are relevant to the early Moon environment. One can calculate the concentrations of VSE resulting in the lunar mantle, $C^i_{sil}$, according to:

$$C^i_{bulk} = x\, C^i_{sil} + (0.985 - x)C^i_{gas} + 0.015C^i_{met}$$

$$C^i_{bulk}/C^i_{sil} = x\ + (0.985 - x)C^i_{gas}/C^i_{sil} + 0.015C^i_{met}/C^i_{sil}$$

$$C^i_{sil} = C^i_{bulk}/\ [x\ + (0.985 - x)D^i_{gas/sil} + 0.015D^i_{met/sil}] \qquad (2)$$

where x is the mass fraction of the Moon that was supplied from a silicate melt phase (so that in the limiting case where all of the Moon’s silicate was derived from the melt, x = 0.985 for a metal core fraction of 0.015), $C^i_{bulk}$ is the bulk composition of the VSE in the Moon (see Stage 1 section), the core fraction is 0.015 from GRAIL constraints [32], and $D^{i}_{met/sil}$ is calculated according to eq. (1) (see Stage 3 section).

### Comparison of observed and calculated mantle concentrations and reconciling volatile depletions with lunar formation models

Using equation (1) and (2) and a *bulk silicate Earth* composition *(PUM)* for the bulk Moon we can examine several hypotheses for the origin of lunar volatiles. Discussion in the main text focuses on a PUM-like bulk Moon because this composition provides successful models for lunar mantle VSE, as will be shown below. The two other Mars-sized impactor mantle bulk compositions do not provide successful models for the lunar mantle VSE and they are described in detail in the **Supplementary information, part 4**.

First, using a PUM composition, without an Earth-Moon volatility correction, unsurprisingly results in lunar mantle VSE concentrations that are too high, indicating the need for depletion mechanisms in addition to Stage 1. High energy lunar formation models produce a gas-rich disk, indicating the melt-gas fractionation may exert a strong control on volatile elements, and can explain the 4x alkali element depletion of the Moon relative to Earth's mantle (3). Assuming that the least volatile element (P) and the most volatile element (Tl) can be explained by gas-melt fractionation with gas fraction of 0.9 and varying the D(gas/melt) from 3 (P) to 100 (Tl) to fit these elements (see **Supplementary information, Table S1**) results in a good match to most of the VSE, but concentrations are still too high for As, Ag, Sb, and Bi – a mismatch of >10 (Stage 2; Figure 2a). It is important to note that all four of these elements are moderately siderophile and thus have a significant depletion due to core formation. When core formation is accounted for (Stage 3), the fit to these four elements is improved, but Ag, Sb, and Bi remain mismatched by ~

10 (Figure 2a). Thus, a scenario of Stages 1, 2 and 3 with a gas-rich stage 2, explains many but not all of the VSE.

Second, lower energy lunar formation scenarios (such as canonical (1) or multiple impact (5) models) might involve mixing between volatile depleted hot inner disk and cooler outer disk (volatile bearing) material which (26) argues can also explain the factor of ~4 depletion of alkali elements in the Moon relative to the Earth. If such mixing caused the overall bulk composition of the Moon to be depleted in volatile elements by ~4x, many VSE can be satisfied (Figure 2b). However, 6 critical VSE (Pb, Zn, Cd, Sn, In, Tl) would remain too high after mixing and require an additional depletion mechanism, since the Stage 3 core formation would not significantly affect these 6 elements (Figure 2b). So, although mixing within the disk can explain many elements, it does not explain the most highly depleted volatiles Pb, Zn, Cd, Sn, In, Tl, and an additional loss mechanism would be required to explain their abundances.

A third scenario offers a hybrid solution that can explain most if not all VSE. If mixing occurred in the early disk, the moderately VSE contents of the bulk Moon may have been set by mixing between the hot inner and cool outer disk (Figure 2c). The greater depletion of the more highly VSE can be caused by temperature dependent gas-melt interactions as the Moon accreted: the six highly VSE may have remained in the gas phase as Moon accretion completed (with gas fraction of 0.5 and D(gas/melt) the same as for scenario 1) (Figure 2c). The transition from these 8 moderately VSE to the 6 more highly VSE at a Tc (50%) ~ 725 K may correspond to an actual temperature near ~1700 K (33,34) (at 1 bar), perhaps reflecting the temperature for the top of the lunar photosphere (i.e., ~2000 K proposed by (35)) . The condensed lunar material would have to segregate from the gas-rich portion of the disk, which could migrate toward or away from Earth; if inward, such late terrestrial accretion would have little effect on Earth's more highly VSE budget, but would leave the Moon severely depleted in these 6 more highly VSEs. Finally, further depletion of the siderophile As, Ag, Sb, and Bi due to core formation, would leave the lunar mantle with a good fit to all 14 VSE (Figure 2c). Thus, volatile elements in the lunar mantle in canonical lunar formation models can be attributed to a combination of volatile depleted pre-cursors, mixing and melt-gas equilibria in the proto-lunar disk, followed by lunar core formation.

## Testing this model and future work

The hybrid scenario, involving both mixing and gas-melt equilibrium, would require a mechanism for gas-melt segregation and currently there are a number of viable possibilities. The combined modelling of Lindblad resonances in the inner disk and N-body simulations of the outer disk material has shown that the Moon accretes from a mixture of hot inner disk material and cooler outer disk material, and that inner gas-rich disk material will ultimately fall back onto Earth (36). Alternatively tidal interactions between the disk and the accreting Moon may cause migration of the forming body outward and away from the gas-rich portions of the disk (35, 36). On the other hand, magneto-hydrodynamic (MHD) modelling has suggested that turbulence-driven viscosity can lead to expansion of gas outward independent of the melt (37) and that post-impact disk volatilization can transport gas ~10 Earth radii outward within several days of the impact (38). Turbulence at the melt-gas interface of a slightly higher pressure disk could move vapor outward as well (39, 40). Finally, the vapor-rich environment of a synestia (3) coupled with disk dynamics offers potential for gas-melt segregation that could represent the more highly VSE identified here. More work on melt-gas dynamics in the proto-lunar disk is obviously required.

Testing of the various Moon formation models for volatile contents has been incomplete, and the current work provides some guidance. Testing the canonical model has only quantitatively included Zn (26), but inclusion of additional elements, and measuring D(VSE) gas/melt, should reveal whether gas-melt dynamics in the lunar disk established the VSE pattern for the bulk silicate Moon. We show above that a lower energy model with a 3 stage process could potentially explain the lunar VSE. More energetic lunar formation models include a collision between a highly spun proto-Earth and impactor that forms a high temperature protolunar disk (2,3), or a direct collision that produces a terrestrial synestia out of which the Moon accretes (3,4). The moderately volatile element depletions may reflect equilibration between disk melt and vapor during cooling at pressures between 10 and 50 bar as was shown for Cu and Zn (3). Calculations for Ge, however, result in values lower than lunar mantle estimates, and also do not account for the siderophile nature of Ge ($D_{metal/silicate} = 50$) which will result in a more severe depletion than previously calculated (3). The ability of the synestia model to account for both the moderately and highly VSE will require examination of more elements. For example, (3) argue that the behavior of some VSE is pressure dependent, but only model Cu, Zn, and Ge which have similar pressure effects. Including more elements will provide more leverage of the pressure dependence – increased pressure causes Ga and Zn to switch their degree of volatility, while Pb becomes more volatile (41). Additionally, the relative volatility of some of the VSE changes if non-ideality is considered (41,42): In, Sb, As, and Bi all become less volatile (and Zn and Ge more volatile).

The close similarity of lunar mantle VSE estimates (from samples) to those calculated assuming bulk Moon is like the terrestrial PUM is supportive of the idea that Moon was derived from the proto-Earth. Our new calculations and assessments utilizing this large group of elements illustrate the degree of volatile depletion across a wide temperature range for the Moon and establish an important baseline for interpreting and evaluating lunar origin models in the future. The effect of core formation on the moderately siderophile VSEs - As, Sb, Ag, Ge, Bi, Sn - must be included in any modeling efforts. The origin of volatiles might also be tested by combining the bulk VSE contents with Ga, Zn, Cl, and K isotopic variation in lunar and terrestrial samples (43-46). Clearly, future modelling that: a) quantifies pre-cursor materials, disk-melt interactions, and core-mantle partitioning, b) includes pressure and non-ideality constraints on melt-gas equilibria for more elements, and c) the strong effects of core formation, is likely to provide important test of lunar formation models for volatile elements. Specifically, the VSE may help to discriminate between lower energy (canonical (1) and multiple impact (5)) and higher energy (synestia (3,4) and sub-Earth (2,3)) models for the origin of the Moon.

## References:

(1) R. M. Canup, Lunar-forming collisions with pre-impact rotation. *Icarus* 196, 518-538 (2008).

(2) R.M. Canup, Forming a Moon with an Earth-like composition via a giant impact. *Science* 338, 1052-1055 (2012).

(3) S.J. Lock, S.T. Stewart, M.I. Petaev, Z. Leinhardt, M.T. Mace, S.B. Jacobsen, M. Cuk, The origin of the Moon within a terrestrial synestia. *Journal of Geophysical Research: Planets 123*, 910-951 (2018); https://doi.org/10.1002/2017JE005333.

(4) M. Ćuk and S.T. Stewart (2012). Making the Moon from a fast-spinning Earth: a giant impact followed by resonant despinning. *Science 338*, 1047-1052.

(5) R. Rufu, O. Aharonson, H.B. Perets, A multiple-impact origin for the Moon. *Nature Geoscience* 10, 89-94 (2017).

(6) A.E. Ringwood, S. Kesson, Composition and origin of the Moon *Proc Lunar Planet Sci Conf* 8, 371-398 (1977);

(7) A.E. Ringwood, Volatile and siderophile element geochemistry of the Moon: a reappraisal. Earth Planet. Sci. Lett. 111, 537-555 (1992).

(8) U. Mann, D.J. Frost, D.C. Rubie, Evidence for high-pressure core-mantle differentiation from the metal–silicate partitioning of lithophile and weakly-siderophile elements. *Geochimica et Cosmochimica Acta* 73, 7360-7386 (2009).

(9) E.S. Kiseeva, B.J. Wood, A simple model for chalcophile element partitioning between sulphide and silicate liquids with geochemical applications. *Earth and Planetary Science Letters* 383, 68-81 (2013).

(10) K. Righter, K. Pando, N. Marin, D.K. Ross, M. Righter, L.R. Danielson, T.J. Lapen, C.T. Lee, Volatile element signatures in the mantles of Earth, Moon, and Mars: Core formation fingerprints from Bi, Cd, In, and Sn. *Meteoritics & Planetary Science* 53, 284-305 (2018).

(11) K. Righter, K. Nickodem, K. Pando, L. Danielson, A. Boujibar, M. Righter, T.J. Lapen, Distribution of Sb, As, Ge, and In between metal and silicate during accretion and core formation in the Earth. *Geochimica et Cosmochimica Acta* 198, 1-16 (2017).

(12) J. Siebert, A. Corgne, F.J. Ryerson, Systematics of metal–silicate partitioning for many siderophile elements applied to Earth’s core formation. *Geochimica et Cosmochimica Acta* 75, 1451-1489 (2011).

(13) M.J. Drake, Trace elements as quantitative probes of differentiation processes in planetary interiors. *Reviews of Geophysics* 18, 11-25 (1980).

(14) Wänke H., Baddenhausen H., Balacescu A., Teschke F., Spettel B., Dreibus G., Palme H., Quijano-Rico M., Kruse H., Wlotzka F., and Begemann F. *Proceedings 3$^{rd}$ Lunar and Planetary Science Conference*, Multi-element analyses of lunar samples and some implications of the results. 1251-1269 (1972).

(15) Wänke, H., Palme, H., Baddenhausen, H., Dreibus, G., Jagoutz, E., Kruse, H., ... & Thacker, R. Chemistry of Apollo 16 and 17 samples-Bulk composition, late stage accumulation and early differentiation of the moon. *Proceedings* 5th *Lunar and Planetary Science Conference*, 1307-1335 (1974).

(16) Wänke, H., Palme, H., Baddenhausen, H., Dreibus, G., Jagoutz, E., Kruse, H., ... & Thacker, R. New data on the chemistry of lunar samples-Primary matter in the lunar highlands and the bulk composition of the moon. *Proceedings* 6th *Lunar and Planetary Science Conference,* 1313-1340 (1975).

(17) Palme, H., Baddenhausen, H., Blum, K., Cendales, M., Dreibus, G., Hofmeister, H., ... & Vilcsek, E. New data on lunar samples and achondrites and a comparison of the least fractionated samples from the earth, the moon and the eucrite parent body. *Proceedings* 9th Lunar *and Planetary Science Conference*, 25-57 (1978).

(18) Wolf R., Woodrow A., and Anders E. Lunar basalts and pristine highland rocks-Comparison of siderophile and volatile elements. *Proceedings* 10th *Lunar and Planetary Science Conference,* 2107-2130 (1979).

(19) Meyer, C.K., Jr. Lunar sample compendium, https://curator.jsc.nasa.gov/lunar/lsc/index.cfm.

(20) N. Dauphas, C. Burkhardt, P.H. Warren, T. Fang-Zhen, T., Geochemical arguments for an Earth-like Moon-forming impactor. *Phil. Trans. R. Soc. A, 372*, p.20130244 (2014).

(21) P.H. Warren, The magma ocean concept and lunar evolution. *Annual Review of Earth and Planetary Sciences 13,* 201-240 (1985).

(22) H. Palme, H.St.C. O'Neill, H. Cosmochemical estimates of mantle composition. In *Treatise on Geochemistry, 2nd Edition*. Elsevier (2014).

(23) J.H. Jones, H. Palme, Geochemical constraints on the origin of the Earth and Moon.in *Origin of the Earth and Moon* (eds. R. Canup and K. Righter), Univ. Arizona Press, Tucson, AZ, 197-216 (2000).

(24) G.J. Taylor, The bulk composition of Mars. *Chemie der Erde-Geochemistry* 73, 401-420 (2013).

(25) S. Yang, M. Humayun, K. Righter, G. Jefferson, D. Fields, A.J. Irving, Siderophile and chalcophile element abundances in shergottites: Implications for Martian core formation. *Meteoritics & Planetary Science* 50, 691-714 (2015).

(26) R.M. Canup, C. Visscher, J. Salmon, B. Fegley Jr, Lunar volatile depletion due to incomplete accretion within an impact-generated disk. *Nature Geoscience* 8, 918-922 (2015).

(27) K. Righter, Does the Moon have a metallic core?: Constraints from giant impact modeling and siderophile elements. *Icarus* 158, 1-13 (2002).

(28) M. Sharp, K. Righter, R.J. Walker, Estimation of trace element concentrations in the lunar magma ocean using mineral- and metal- silicate melt partition coefficients. *Meteoritics & Planetary Science* 50, 733-758 (2015).

(29) E.S. Steenstra, N. Rai, J.S. Knibbe, Y.H. Lin, W. van Westrenen, W., New geochemical models of core formation in the Moon from metal–silicate partitioning of 15 siderophile elements. *Earth and Planetary Science Letters* 441, 1-9 (2016).

(30) K. Righter, L.R.. Danielson, K.M. Pando, G.A. Shofner, S.R. Sutton, M. Newville, C.T. Lee, Valence and metal/silicate partitioning of Mo: Implications for conditions of Earth accretion and core formation. *Earth and Planetary Science Letters* 437, 89-100 (2016).

(31) J.D. Kendall, H.J. Melosh, Differentiated planetesimal impacts into a terrestrial magma ocean: Fate of the iron core. *Earth and Planetary Science Letters* 448, 24-33 (2016).

(32) J.G. Williams, A.S. Konopliv, D.H. Boggs, R.S. Park, D.N. Yuan, F.G. Lemoine, S. Goossens, E. Mazarico, F. Nimmo, R.C. Weber, S.W. Asmar, Melosh, H.J., Neumann, G.A., Phillips, R.J., Smith, D.E., Solomon, S.C., Watkins, M.M., Wieczorek, M.A., Andrews-Hanna, J.C., Head, J.W., Kiefer, W.S., Matsuyama, I., McGovern, P.J., Taylor, G.J., and Zuber, M.T., Lunar interior properties from the GRAIL mission. *Journal of Geophysical Research: Planets* 119, 1546-1578 (2014).

(33) K. Lodders, Solar system abundances and condensation temperatures of the elements. *The Astrophysical Journal 591*, 1220-1240 (2003).

(34) P. Sossi, S. Klemme, H. St.C. O'Neill, J. Berndt, F. Moynier, Experimental constraints on the evaporation of moderately volatile elements during planetary formation, Goldschmidt meeting Abstract, #3729 (2017).

(35) W.R. Ward, On the evolution of the protolunar disc. *Phil. Trans. R. Soc. A* 372, 20130250 (2014).

(36) J. Salmon, R.M. Canup, Lunar accretion from a Roche-interior fluid disk. *The Astrophysical Journal* 760, 83-95 (2012).

(37) A. Carballido, S.J. Desch, G.J. Taylor, Magneto-rotational instability in the protolunar disk. *Icarus* 268, 89-101 (2016).

(38) C.F. Gammie, W.T. Liao, P.M. Ricker, A hot big bang theory: Magnetic fields and the early evolution of the protolunar disk. *The Astrophysical Journal* 828, 58-68 (2016).

(39) S. Charnoz, C. Michaut, Evolution of the protolunar disk: Dynamics, cooling timescale and implantation of volatiles onto the Earth. *Icarus 260*, 440-463 (2015).

(40) W.R. Ward, On the vertical structure of the protolunar disk. *The Astrophysical Journal* 744, 140-152 (2012).

(41) L. Schaefer, B. Fegley, Volatile element chemistry during metamorphism of ordinary chondritic material and some of its implications for the composition of asteroids. *Icarus* 205, 483-496 (2010).

(42) C.A. Norris, B.J. Wood, Earth's volatile contents established by melting and vaporization. *Nature* 549, 507-510 (2017).

(43) K. Wang, S.B. Jacobsen, Potassium isotopic evidence for a high-energy giant impact origin of the Moon. *Nature* 538, 487-89 (2016).

(44) C. Kato, F. Moynier, Gallium isotopic evidence for extensive volatile loss from the Moon during its formation. *Science Advances* 3, p.e1700571 (2017).

(45) R.C. Paniello, J.M. Day, F. Moynier, Zinc isotopic evidence for the origin of the Moon. *Nature* 490, 376-379 (2012).

(46) Z.D. Sharp, C.K. Shearer, K.D. McKeegan, J.D. Barnes, Y.Q. Wang, The chlorine isotope composition of the Moon and implications for an anhydrous mantle. *Science* 329, 1050-1053 (2010).

**Supplementary information references:**

(47) Wänke H. and Dreibus G. 1986. Geochemical evidence for the formation of the Moon by impact-induced fission of the proto-Earth. In *Origin of the Moon,* Proceedings of the Conference, Kona, HI, October 13-16, Eds. W. K. Hartmann, R. J. Phillips, and G. J. Taylor, p. 649-671.

(48) Righter K., Chesley J. T., Caiazza C. M., Gibson E. K., and Ruiz J. 2008. Re and Os concentrations in arc basalts: The roles of volatility and source region $fO_2$ variations. *Geochimica et Cosmochimica Acta* 72, 926-947.

(49) Danckwerth, P. A., Hess, P. C., and Rutherford, M. J. 1979. The solubility of sulfur in high-$TiO_2$ mare basalts. In 10th *Lunar and Planetary Science Conference Proceedings*, 517-530.

(50) Gibson Jr, E. K., Brett, R., & Andrawes, F. 1977. Sulfur in lunar mare basalts as a function of bulk composition. In 8th *Lunar and Planetary Science Conference Proceedings*, 1417-1428.

(51) Rubin, K. 1997. Degassing of metals and metalloids from erupting seamount and mid-ocean ridge volcanoes: Observations and predictions. *Geochimica et Cosmochimica Acta* 61, 3525-3542.

(52) Saal, A.E., Hauri, E.H., Cascio, M.L., Van Orman, J.A., Rutherford, M.C. and Cooper, R.F. 2008. Volatile content of lunar volcanic glasses and the presence of water in the Moon's interior. *Nature* 454, 192.

(53) McKay, D.S. and Wentworth, S.J. 1992. Morphology and composition of condensates on Apollo 17 orange and black glass. Lunar Science Inst., Workshop on Geology of the Apollo 17 Landing Site, p. 31-36.

(54) Meyer Jr, C., McKay, D. S., Anderson, D. H., & Butler Jr, P. 1975. The source of sublimates on the Apollo 15 green and Apollo 17 orange glass samples. *Proceedings* 6th *Lunar and Planetary Science Conference*, 1673-1699.

(55) Herzog, G.F., Moynier, F., Albarède, F., and Berezhnoy, A.A. 2009. Isotopic and elemental abundances of copper and zinc in lunar samples, Zagami, Pele's hairs, and a terrestrial basalt. *Geochimica et Cosmochimica Acta* 73, 5884-5904.

(56) Renggli, C. J., King, P. L., Henley, R. W., & Norman, M. D. 2017. Volcanic gas composition, metal dispersion and deposition during explosive volcanic eruptions on the Moon. *Geochimica et Cosmochimica Acta 206*, 296-311.

(57) Shearer, C.K., Papike, J.J., Simon, S.B., Shimizu, N., Yurimoto, H., and Sueno, S. 1990. Ion microprobe studies of trace elements in Apollo 14 volcanic glass beads: Comparisons to Apollo 14 mare basalts and petrogenesis of picritic magmas. *Geochimica et Cosmochimica Acta* 54, 851-867.

(58) Dickinson, T., Taylor, G.J., Keil, K., and Bild, R.W. 1989. Germanium abundances in lunar basalts-Evidence of mantle metasomatism?. *Proceedings 19th Lunar and Planetary Science Conference*, 189-198.

(59) Newsom, H. E. 1986. Constraints on the origin of the Moon from the abundance of molybdenum and other siderophile elements. In *Origin of the Moon*, Proceedings of the Conference, Kona, HI, October 13-16, Eds. W. K. Hartmann, R. J. Phillips, and G. J. Taylor, p. 203-229.

(60) Basaltic Volcanism Study Project 1981. *Basaltic Volcanism on the Terrestrial Planets*. Pergamon Press, 1282 pp.

(61) Brunfelt, A. O., Heier, K. S., & Steinnes, E. 1971. Determination of 40 elements in Apollo 12 materials by neutron activation analysis. In 2nd *Proceedings of the Second Lunar Science Conference*, 1281-1290.

(62) Wänke H., Rieder R., Baddenhausen H., Spettel B., Teschke F., Quijanorico M., and Balacescu A. 1970. Major and trace elements in lunar material. *1st Proceedings Lunar and Planetary Science Conference*, 1719-1736.

(63) Wänke H., Wlotzka F., Baddenhausen H., Balacescu A., Spettel B., Teschke F., Jagoutz E., Kruse H., Quijano-Rico M., and Rieder R. 1971. Apollo 12 samples: Chemical composition and its relation to sample locations and exposure ages, the two-component origin of the various soil samples and studies on lunar metallic particles. *Proceedings 2nd Lunar and Planetary Science Conference*, 1187-1199.

(64) Wänke H., Baddenhausen H., Dreibus G., Jagoutz E., Kruse H., Palme H., Spettel B., and Teschke F. 1973. Multi-element analyses of Apollo 15, 16 and 17 samples and the bulk composition of the Moon. *Proc. 4th Lunar Sci. Conf. , 1*461–1481.

(65) Wänke, H., Baddenhausen, H., Blum, K., Cendales, M., Dreibus, G., Hofmeister, H., ... & Thacker, R. 1977. On the chemistry of lunar samples and achondrites-Primary matter in the lunar highlands: A re-evaluation. In *Proceedings* 8th *Lunar and Planetary Science Conference.* 2191-2213.

(66) Snyder, G. A., Neal, C. R., Taylor, L. A., & Halliday, A. N. 1997. Anatexis of lunar cumulate mantle in time and space: Clues from trace-element, strontium, and neodymium isotopic chemistry of parental Apollo 12 basalts. *Geochimica et Cosmochimica Acta* 61, 2731-2747.

(67) Ryder, G., and Schuraytz, B.C. 2001. Chemical variation of the large Apollo 15 olivine-normative mare basalt rock samples. *Journal of Geophysical Research: Planets 106*(E1), 1435-1451.

(68) Taylor S. R., Rudowski R., Muir P., Graham A., and Kaye M. 1971. Trace element chemistry of lunar samples from the Ocean of Storms. *Proceedings* 2nd *Lunar and Planetary Science Conference*, 1083-1099.

(69) Warren, P. H., Shirley, D. N., & Kallemeyn, G. W. 1986. A potpourri of pristine Moon rocks, including a VHK mare basalt and a unique, augite-rich Apollo 17 anorthosite. *Journal of Geophysical Research: Solid Earth 91*, 319-330.

(70) Norman, M. D., Adena, K. J. D., & Christy, A. G. 2012. Provenance and Pb isotopic ages of lunar volcanic and impact glasses from the Apollo 17 landing site. *Australian Journal of Earth Sciences* 59, 291-306.

(71) Albarède, F., Albalat, E., & Lee, C. T. A. 2015. An intrinsic volatility scale relevant to the Earth and Moon and the status of water in the Moon. *Meteoritics & Planetary Science* 50, 568-577.

(72) Hauri, E. H., Saal, A. E., Rutherford, M. J., & Van Orman, J. A. 2015. Water in the Moon's interior: Truth and consequences. *Earth and Planetary Science Letters* 409, 252-264.

(73) Morgan, J. W., Wandless, G. A., Petrie, R. K., & Irving, A. J. 1980. Composition of the earth's upper mantle. II-Volatile trace elements in ultramafic xenoliths. In 11th *Lunar and Planetary Science Conference Proceedings*, 213-233.

(74) Hertogen J., Janssens M. J., and Palme H. 1980. Trace elements in ocean ridge basalt glasses: implications for fractionations during mantle evolution and petrogenesis. *Geochimica et Cosmochimica Acta* 44, 2125-2143.

(75) Jochum K. P., Hofmann A. W., and Seufert H. M. 1993. Tin in mantle-derived rocks: constraints on Earth evolution. *Geochimica et Cosmochimica Acta* 57, 3585-3595.

(76) Yi W., Halliday A. N., Lee D. C., and Christensen J. N. 1995. Indium and tin in basalts, sulfides, and the mantle. *Geochimica et Cosmochimica Acta* 59, 5081-5090.

(77) Yi W., Halliday A. N., Alt J. C., Lee D. C., Rehkämper M., Garcia M. O., and Su, Y. 2000. Cadmium, indium, tin, tellurium, and sulfur in oceanic basalts: Implications for chalcophile

element fractionation in the Earth. *Journal of Geophysical Research: Solid Earth* 105, 18927-18948.

(78) Norman M.D., Garcia M.O., and Bennett V.C. 2004. Rhenium and chalcophile elements in basaltic glasses from Ko'olau and Moloka'i volcanoes: Magmatic outgassing and composition of the Hawaiian plume. *Geochimica et Cosmochimica Acta* 68, 3761-3777.

(79) Witt-Eickschen G., Palme H., O'Neill H. S. C., and Allen C. M. 2009. The geochemistry of the volatile trace elements As, Cd, Ga, In and Sn in the Earth's mantle: new evidence from in situ analyses of mantle xenoliths. *Geochimica et Cosmochimica Acta* 73, 1755-1778.

(80) Jenner F.E., Arculus R.J., Mavrogenes J.A., Dyriw N.J., Nebel O., and Hauri E.H. 2012. Chalcophile element systematics in volcanic glasses from the northwestern Lau Basin. *Geochemistry, Geophysics, Geosystems 13(6)*.

(81) Jochum K. P., Weis U., Schwager B., Stoll B., Wilson S. A., Haug G. H., Andreae M. O. and Enzweiler J. 2016. Reference Values Following ISO Guidelines for Frequently Requested Rock Reference Materials. *Geostand. Geoanal. Res.* 40, 333–350. doi:10.1111/j.1751-908X.2015.00392.x

(82) Johnson, A. and Canil, D. 2011. The degassing behavior of Au, Tl, As, Pb, Re, Cd and Bi from silicate liquids: Experiments and applications. *Geochimica et Cosmochimica Acta* 75, 1773-1784.

(83) Moynier, F., Albarède, F., & Herzog, G. F. 2006. Isotopic composition of zinc, copper, and iron in lunar samples. *Geochimica et Cosmochimica Acta 70*, 6103-6117.

(84) Humayun, M., DiFrancesco, N., & Ustunisik, G. 2016. Experimental Confirmation of the Volatility of Germanium in Martian Basalts. In *79th Annual Meeting of the Meteoritical Society*, LPI Contrib. No. 1921, #6491.

(85) Ustunisik, G., DiFrancesco, N., Yang, S., Humayun, M., and Rogaski, A. 2018. Role of Cl and S on the Volatility of Ge, Zn, and Li in Martian Basaltic Magmas: Implications for Volatile Contribution to Martian Surface Lithologies. In 49th *Lunar and Planetary Science Conference,* #2659.

(86) Taylor, G. J., & Wieczorek, M. A. 2014. Lunar bulk chemical composition: a post-Gravity Recovery and Interior Laboratory reassessment. *Phil. Trans. R. Soc. A*, *372*(2024), 20130242.

(87) Turcotte, D.L., and G. Schubert 1982. Geodynamics: Applications of continuum physics to geological problems, John Wiley and Sons, New York, 450 pp.

(88) Newsom H. E. 1995. Composition of the solar system, planets, meteorites, and major terrestrial reservoirs. *Global Earth Physics*, 159-189.

(89) Neal C.R. 2001. Interior of the Moon: The presence of garnet in the primitive deep lunar mantle. *J. Geophys. Res.* 106, 27865-27885.

(90) Tatsumoto M., Knight R.J., and Doe B.R. 1971. U-Th-Pb systematics of Apollo 12 lunar samples. *Proc. Lunar Sci. Conf. 2nd*, 1521-1546.

(91) Tatsumoto M., Premo W.R., and Unruh D.M. 1987. Origin of lead from Green Glass of Apollo 15426: A search for primitive lunar lead. Proc. Lunar Planet. Sci. Conf 17th, in *J. Geophys. Res.* 92, E361-E371.

(92) Nunes P.D., Tatsumoto M., and Unruh D.M. 1974. U-Th-Pb systematics of some Apollo 17 lunar samples and implications for a lunar basin excavation chronology. *Proc. Lunar Sci. Conf.* 5th, 1487-1514.

(93) Nunes P.D. and Tatsumoto M. 1975. U-Th-Pb systematics of selected samples from Apollo 17, Boulder 1, Station 2. *The Moon* 14, 463-471.

(94) Tilton G.R. and Chen J.H. 1979. Lead isotope systematics of three Apollo 17 mare basalts. *Proc. Lunar Planet. Sci. Conf.* 10th, 259-274.

(95) Jenner F. E., and O'Neill H.S.C. 2012. Analysis of 60 elements in 616 ocean floor basaltic glasses. *Geochemistry, Geophysics, Geosystems 13*(2).

(96) Lodders, K. and Fegley Jr, B. 1997. An oxygen isotope model for the composition of Mars. *Icarus* 126, 373-394.

(97) Righter, K., Pando, K., Humayun, M., Waeselmann, N., Yang, S., Boujibar, A., and Danielson, L.R. 2018. Effect of Silicon on Activity Coefficients of Siderophile Elements (Au, Pd, Pt, P, Ga, Cu, Zn, and Pb) in Liquid Fe: Roles of Core Formation and a Late Sulfide Matte in Shaping Terrestrial Mantle Geochemistry. *Geochimica et Cosmochimica Acta* 232, 101-123.

(98) Righter, K., Pando, K., Ross, D.K., Righter, M., and Lapen, T.J. 2018. Effect of Silicon on Activity Coefficients of P, Bi, Cd, Sn, and Ag in Liquid Fe-Si, and Implications for Core Formation, 49th Lunar and Planetary Science Conference, #2471.

(99) Wood, B. J., Nielsen, S. G., Rehkämper, M., & Halliday, A. N. 2008. The effects of core formation on the Pb-and Tl-isotopic composition of the silicate Earth. *Earth and Planetary Science Letters 269*, 326-336.

(100) Nielsen, S. G., N. Shimizu, C.-T. A. Lee, and M. D. Behn 2014. Chalcophile behavior of thallium during MORB melting and implications for the sulfur content of the mantle, *Geochem. Geophys. Geosyst.*, 15, 4905–4919, doi:10.1002/2014GC005536.

(101) Magna, T., Wiechert, U., & Halliday, A. N. 2006. New constraints on the lithium isotope compositions of the Moon and terrestrial planets. *Earth and Planetary Science Letters 243*, 336-353.

(102) Herd, C. D., Treiman, A. H., Mckay, G. A., & Shearer, C. K. 2004. The behavior of Li and B during planetary basalt crystallization. *American Mineralogist* 89, 832-840.

**Acknowledgements:** Support for this research was provided by RTOPs from the NASA LASER and Cosmochemistry programs, and NASA's Planetary Science Research Program. Lunar sample data was navigated with the aid of Chuck Meyer's Lunar Sample Compendium and Clive Neal's Lunar List Serve Mare Basalt Database. Discussions with Jeff Taylor, Marc Norman, Sasha Nemchin, and Clive Neal were beneficial to interpreting some of the elemental data. All data needed to evaluate the conclusions in the paper are present in the paper and/or the Supplementary Materials. Additional data related to this paper may be requested from the authors. The author declares that he has no competing interests.

## List of Supplementary Materials

### Supplementary Materials

Supplementary Information text (parts 1-4), including Table S1, Figures S1-S5, and references

Supplementary Extended Data file (excel format)

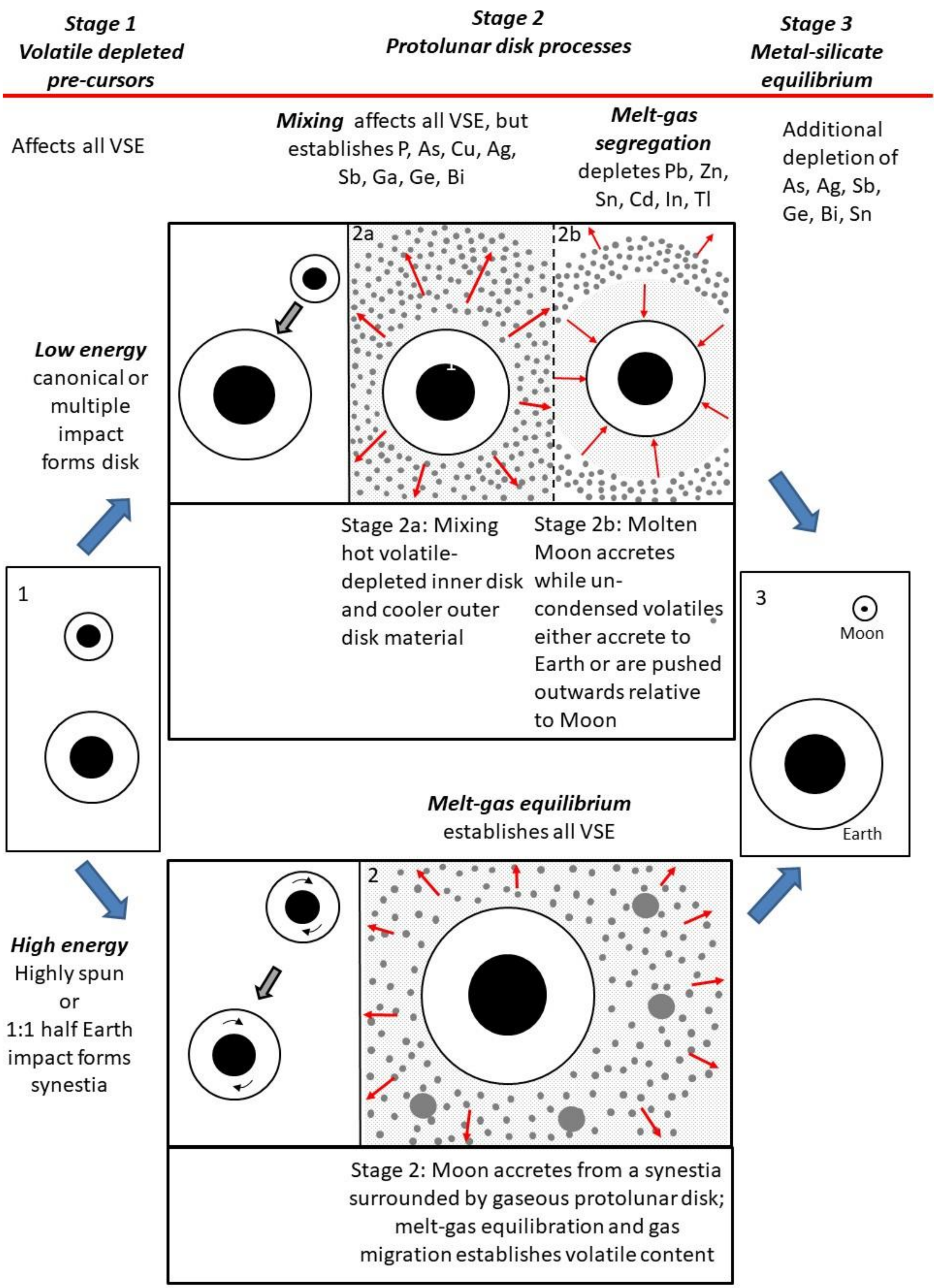
Stage 1
Volatile depleted pre-cursors
Stage 2
Protolunar disk processes
Stage 3
Metal-silicate equilibrium
Affects all VSE
Mixing affects all VSE, but establishes P, As, Cu, Ag, Sb, Ga, Ge, Bi
Melt-gas segregation depletes Pb, Zn, Sn, Cd, In, Tl
Additional depletion of As, Ag, Sb, Ge, Bi, Sn
Low energy canonical or multiple impact forms disk
2a
2b
Stage 2a: Mixing hot volatile-depleted inner disk and cooler outer disk material
Stage 2b: Molten Moon accretes while un-condensed volatiles either accrete to Earth or are pushed outwards relative to Moon
1
3
Moon
Earth
Melt-gas equilibrium establishes all VSE
High energy Highly spun or 1:1 half Earth impact forms synestia
2
Stage 2: Moon accretes from a synestia surrounded by gaseous protolunar disk; melt-gas equilibration and gas migration establishes volatile content

**Figure 1:** Schematic illustration of the stages proposed to explain the volatile element concentrations in the lunar mantle. Stage 1 is the initial volatile depleted pre-cursor material. In this study three different bulk Moon compositions are considered – terrestrial PUM, a Mars-sized impactor mantle that less volatile depleted than PUM, and a Mars-sized impactor that is more volatile depleted than PUM. Stage 2 has two possible scenarios depicted in the top and bottom panels. In the top panel, Stage 2a is caused by mixing of hot volatile-depleted inner disk material with cooler volatile-bearing outer disk material in the post impact protolunar disk. Stage 2b is the segregation of melt and gas in the protolunar disk, which depleted the Moon of volatile elements with Tc (50%) < ~725 K and may correspond to an actual temperature near ~1700 K (33,34) (at 1 bar), perhaps reflecting the temperature for the top of the lunar photosphere (i.e., ~2000 K proposed by (35)) The pattern of volatile element depletion may thus reflect the thermal structure of the protolunar disk or a quasi-steady state temperature at the top of the photosphere (40). Remaining gas might move inward or outward depending on the driving physical mechanism. In the bottom panel, Stage 2 is a simple gas-melt equilibrium such as may exist in a terrestrial synestia (3). Finally, Stage 3 is the formation of the lunar core which further depleted the most siderophile elements As, Ag, Sb, Ge, Bi and Sn. This multi-stage model can potentially provide a quantitative explanation for these 14 VSE as well as lithophile volatile elements Li, Na, K, Rb, and Cs, but needs to be tested for specific lunar formation models (see detailed discussion in the text).

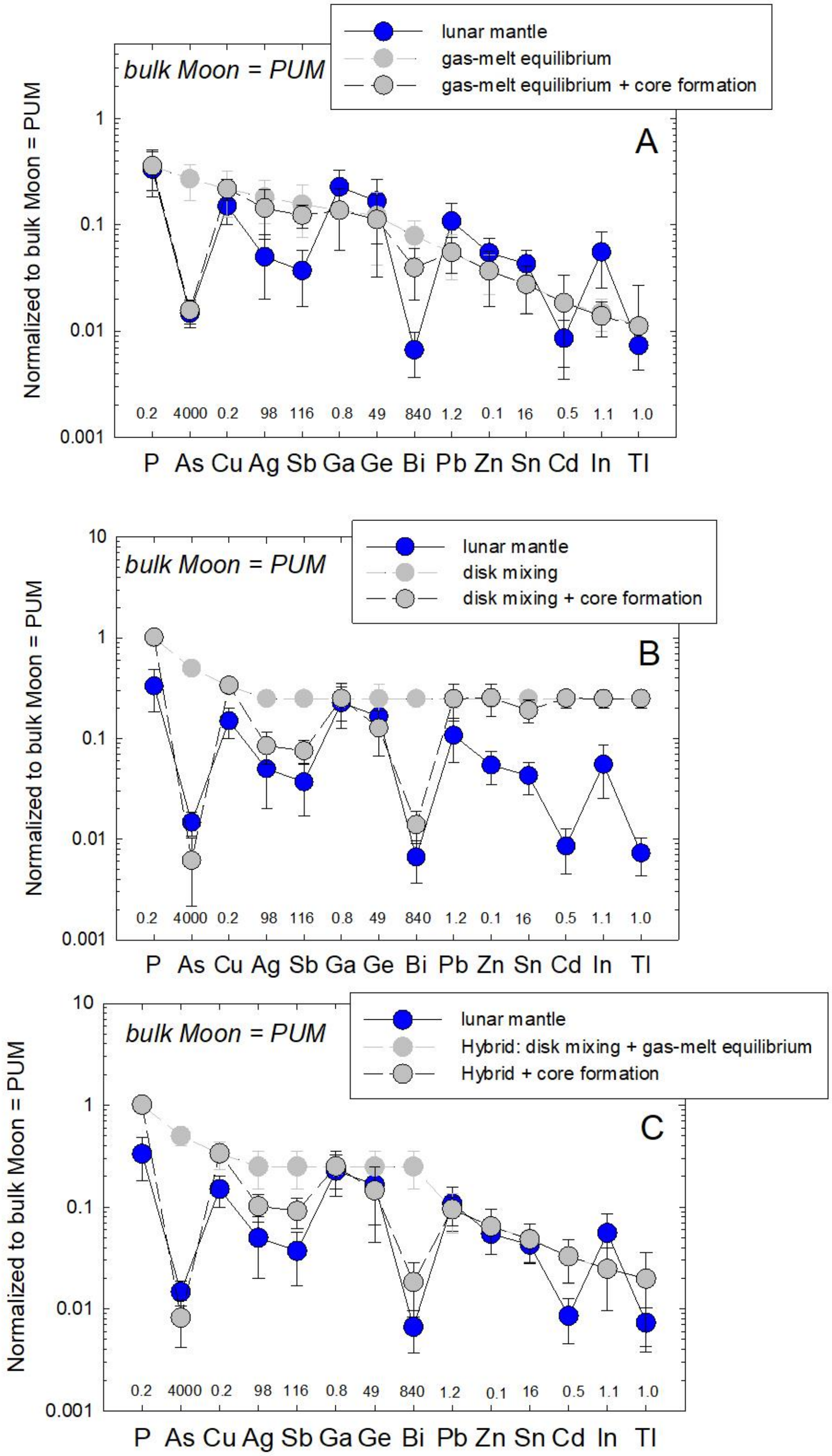

**Figure 2:** Fourteen volatile siderophile elements listed in the order of volatility as gauged by their 50% condensation temperature from [33]. Blue symbols are lunar mantle estimates from correlations between the VSE and a refractory lithophile element (RLE) (see Supplementary Information

part 1). Three panels illustrate the three scenarios discussed in the text – gas-melt equilibrium followed by core formation, disk mixing followed by core formation, and a combination of gas-melt and disk mixing followed by core formation. All calculations assume a bulk Moon composition that is Earth's primitive upper mantle (PUM).

**A)** shows calculated lunar mantle if set by gas-melt equilibrium (light grey circles) followed by core formation (heavier grey circles). Gas-melt equilibrium is calculated using equation 2 with gas fraction = 0.9, and D(gas/melt) set for P= 3 (least volatile) and Tl = 100 (most volatile), and varied as a simple linear function for elements of intermediate volatility. For this scenario, Ag, Sb, and Bi are poor fits, while most other elements fit well.

**B)** shows the calculated mantle if set by mixing between hot inner disk and cooler volatile-bearing outer disk (as per (26); light grey circles) followed by core formation (heavier grey circles). Most of the moderately volatile siderophile elements are fit well in this scenario, but the higher volatility Pb, Zn, Sn, Cd, In, and Tl are overabundant compared to the observed mantle concentrations.

**C)** shows the calculated lunar mantle for a hybrid model of combined disk mixing and gas-melt segregation (grey circles) followed by core formation (heavier grey circles). The gas fraction in this model is 0.5, and the gas/melt partition coefficients the same as for the first scenario (and summarized in Table S1). This model fits all 14 elements well, including the Ag, Sb, and Bi contents that were not fit well in the first scenario.

Values above the elements on the x-axis are the metal/silicate partition coefficients calculated for lunar core formation conditions. Note the high metal/silicate partition coefficient values for As, Ag, Sb, Ge, Bi, and Sn reflecting more siderophile behavior, whereas P, Cu, Ga, Pb, Zn, Cd, In, and Tl are ≤1 reflecting their more lithophile behavior.

# Supplementary Information (Righter, "Volatile element depletion of the Moon – the roles of pre-cursors, post-impact disk dynamics, and core formation")

## 1 - Lunar mantle concentrations of the volatile siderophile elements (VSE)

Because we have no direct samples of the lunar mantle, siderophile element concentrations in the Moon's mantle must be estimated from values measured in mantle melts (lunar basalts and volcanic glasses). During melting of the mantle, the distribution of an element between solid and liquid can be monitored with the partition coefficient, $D$, which is the weight ratio of an element between a solid phase and silicate melt. Elements exhibit either compatible ($D > 1$) or incompatible ($D < 1$) behavior, so that compatible elements have lower concentrations in melts and incompatible elements have higher concentrations in melts, compared to the mantle. Correlations between a siderophile element and refractory lithophile element of equal compatibility or incompatibility will not be fractionated significantly during mantle melting and magmatic crystallization processes (e.g., high versus low Ti basalts for the Moon, or ocean island basalt, mid ocean ridge basalt or komatiite for Earth) and thus can be used to estimate concentrations of siderophile elements in the original mantle.

This approach was pioneered by (47) who showed that the Co and Ni concentrations (both compatible) in the lunar mantle could be estimated from correlations with Mg and Fe. In addition, many refractory siderophile elements are incompatible during melting of a metal-free mantle (e.g., Mo, W, and P; (47)), and when coupled with a refractory lithophile element of nearly equal incompatibility (e.g., La or Nd), their correlation can be used to estimate the original mantle concentration (Fig. S1). For refractory and moderately siderophile elements, the correlation line is well below the chondritic siderophile element values (at a given refractory lithophile element abundance), and this "depletion" relative to chondrites is due to metal–silicate equilibrium (core formation) in that particular body. Hypothetical planets (A, B, C, etc.) would then have slightly different depletions of siderophile elements (Fig. S1). Exceptions to this occur when either metal or sulfide are present in the mantle source, or if degassing has affected the siderophile element. If metal is present in the mantle during melting, the concentration of the siderophile element will be fixed or buffered at variable refractory lithophile element concentrations (Fig. S1); metal does not affect the elements considered here, however, because none of the correlations discussed below are flat. Variable amounts of sulfide in the source can affect the concentrations of chalcophile elements during melting (e.g., (48)), but the Moon is thought to be S poor and S-undersaturated such that there would be no residual sulfide in the mantle (e.g., (49,50)). Finally, some volatile siderophile elements such as Cu, As, Sb, Ge, Pb, and Zn exhibit a range of concentrations at any given RLE concentration (e.g., Ti, Pr, or Ti), which is a reflection of magmatic degassing that may affect these elements more strongly than others (although the concentrations of these elements exhibit large ranges that are likely due to degassing, equally expected from emanation coefficients (51), severe depletions of Bi, Ag, and Sn are not observed). For those elements, then, we choose the highest concentrations in basalts (and glasses where appropriate but see next paragraph) as reflecting an undegassed melt or melting product, and thus representative of the lunar mantle.

Lunar volcanic glasses deserve some detailed discussion, as their volatile contents can have a more complicated history. Because lunar volcanic glasses are typically small melt droplets, diffusion can affect the concentrations in glasses, with diffusive loss being substantial (e.g., (52)). On the other hand volatiles can condense from gases, with condensation being dependent upon the composition of the gas (e.g., Cl or S rich), such that volcanic condensates can be enriched in volatile elements as well (53,54,55,56). Because of these factors, volcanic glass data are used very carefully and sparingly in the analysis here. For example, Cu and Zn both show a wide range of concentrations in volcanic glasses, most likely due to effects of volcanic processing; some are low due to degassing, while others are high due to condensation (54, 57). Germanium is highly susceptible to such volcanic enrichment and depletion processes, as shown in the dataset of (58).

The siderophile element abundances discussed in this work have all been estimated in the manner pioneered by (47) (see also (59) for a summary of this approach), with the important caveats and cautions discussed above regarding volcanic processes and the lunar glass data. For all lunar samples, samples plotted are pristine (not brecciated) and so they record levels unaffected by chondritic contamination. Data for specific elements are discussed in detail below, and lunar mantle estimates are presented using the data in Figs. S2.

### *P, As, Cu, Sb, Ga, Zn*

Sb, As, Ga, Ge, P, Cu, and Zn mantle estimates are determined using correlations with an appropriately matched lithophile element. Sources for these data include basaltic rocks reported by (29-33, 60-69), and glasses reported by (70-72). Terrestrial data are from (60, 73-81).

P correlations with La are maintained over a wide range of P and La contents which makes the interpretation straightforward and uncertainty lower. There is no evidence for significant degassing of P, with the exception of one set of pyroclastic glass data that are not used in the P mantle estimates. As and Sb data are sparse and also exhibit a range of As and Sb contents suggesting that the lowest values may result from degassing. This is consistent with emanation coefficient data (51) and diffusivity data (82) for As and Sb suggesting magmatic volatility is an important influence. The range at the highest values represents a best estimate of the least degassed liquids. Cu, Ga and Zn have similar behavior and for all three elements the correlations are defined using data from both glasses and basalts. Some of the highest values reported for samples that are obviously associated with volcanic processes causing enrichment (55, 57, 83) have not been included because the abundances of these elements are known to be enriched and redistributed during magmatic degassing, plumes and recondensation (53, 54, 56). In summary, the mantle concentration ranges determined here are based on a best estimate of the least degassed liquids, the main assumptions for which are that elements such as Cu and Zn are known to be redistributed during pyroclastic events, and that Sb and As are susceptible to magmatic degassing.

### *Ag*

Ag data from Apollo 12, 14, 15, 16 and 17 basalts of (33) are used to estimate the Ag content of the lunar mantle = 0.2(1) ppb. As with Cu, Ga, and Zn, the highest values are interpreted as undegassed, and thus representing melts from the mantle. The lowest Ag values were not used to estimate the mantle Ag contents because they have likely been compromised from degassing processes.

### *Ge*

For Ge only a few datasets are available (33, 58, 63, and 71). Ge is known to be volatile during magmatic processes, with enhanced volatility in Cl-rich systems, and is also suspected to be volatile in martian magmas (84, 85). As a result, Ge may be susceptible to enrichment in fumarolic activity and pyroclastic processes (58), and it may be lost from magmas (33, 58). In this work, the highest Ge values (near 1 ppm) are not used for reconstructing mantle Ge contents because they are likely enriched in magmatism or fumarolic activity. The lowest values have been likely caused by Ge loss from magmas. As a result the Ge mantle estimates are based on the intermediate values measured in a wide range of both glasses and basalts in Apollo 11, 12 and 15 basalts (63, 71).

*Bi, Sn, Cd, In, and Tl*

Depletions of Sn, Bi, In, and Cd in the lunar mantle were defined in (10) and will not be described in detail again; the reader is referred to that work for a detailed description of data and approaches used. The Cd and In contents are defined by a narrow range of concentrations, and interpretation is straightforward. However, Bi and Sn exhibit a slightly wider range, and the interpretation is similar to that for Cu, Ga, Zn and Ag – slight degassing results in the lowest values which are not used in reconstructing the mantle concentrations of Bi and Sn. Thallium in the lunar mantle was estimated by (86) and their work is adopted here.

*Pb*

Pb-Ce correlations are used to estimate Pb content of the lunar mantle. Pb poses a special case because $^{206}$Pb, $^{207}$Pb, and $^{208}$Pb derived from decay of $^{232}$Th, $^{235}$U, and $^{238}$U. For a 3.2 to 3.7 Ga age basalt, Pb concentrations must be corrected for decay of U and Th. Using the expressions $^{206}\mathrm{Pb} = {}^{232}\mathrm{Th} * e(\lambda t\text{-}1)$, $^{207}\mathrm{Pb} = {}^{235}\mathrm{U} * e(\lambda t\text{-}1)$, $^{208}\mathrm{Pb} = {}^{238}\mathrm{U} * e(\lambda t\text{-}1)$, U, Th, and Pb concentrations from the data sources described in Figure S2, and ages of 3.2 Ga for Apollo 12 and Apollo 15 basalts and 3.7 Ga for Apollo 17 basalts (e.g., 34), and decay constants from (87), the Pb concentrations are corrected for radioactive decay of U and Th. For most samples the remaining Pb is from 1-2% to ~70% of the original measured Pb.

Estimates for all 14 elements are summarized in Table S1 and compare favorably with previous estimates such as (72) and (86). Some exceptions where slight differences in estimated value exist are Zn: we estimate 3 ± 2 ppm Zn compared to the estimate of 7.7 ppm (72). And we estimate 0.25 ppb Sb compared to 0.02 ppb (86), for example. These differences can likely be attributed to use of slightly different datasets and assumptions about degassing.

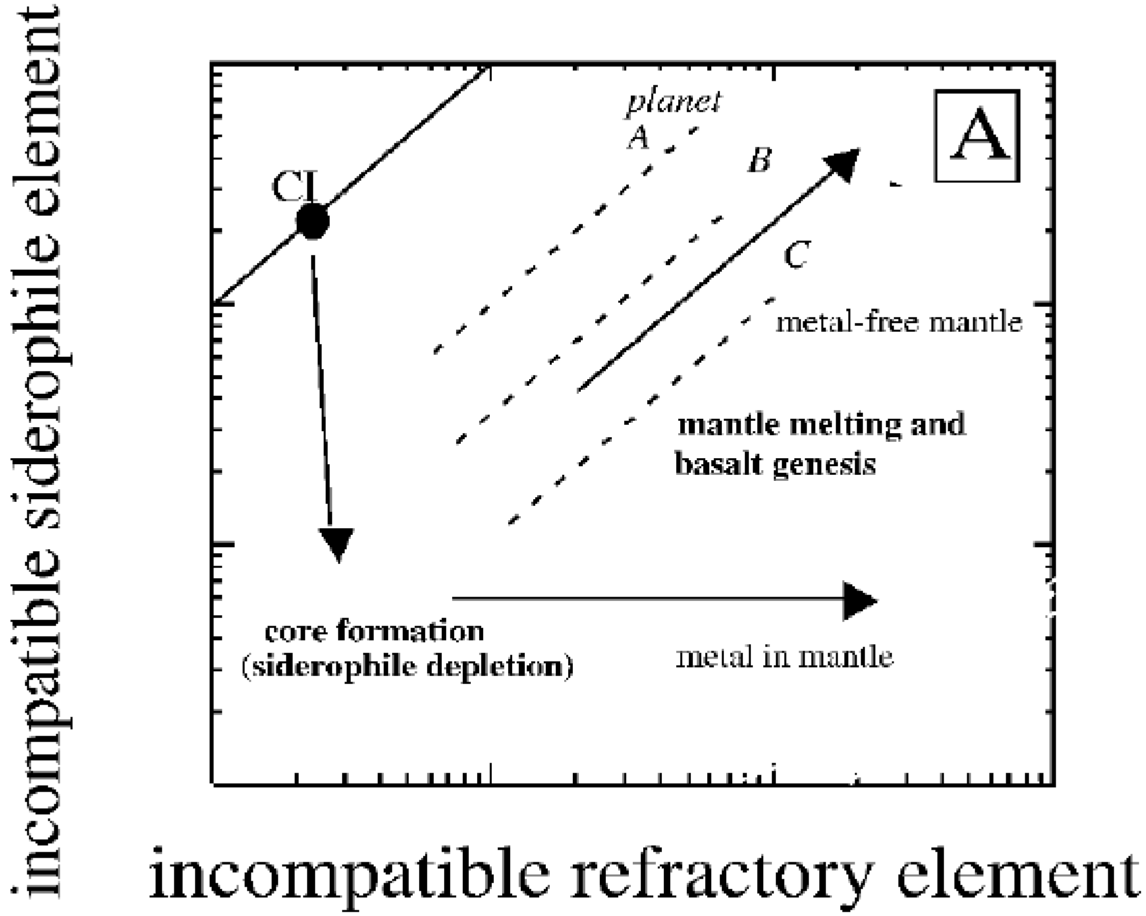

**Figure S1:** hypothetical behavior of a siderophile – refractory lithophile element pair during mantle melting and subsequent processes (trapped metal, residual sulfide and later degassing). Figure adapted from (41).

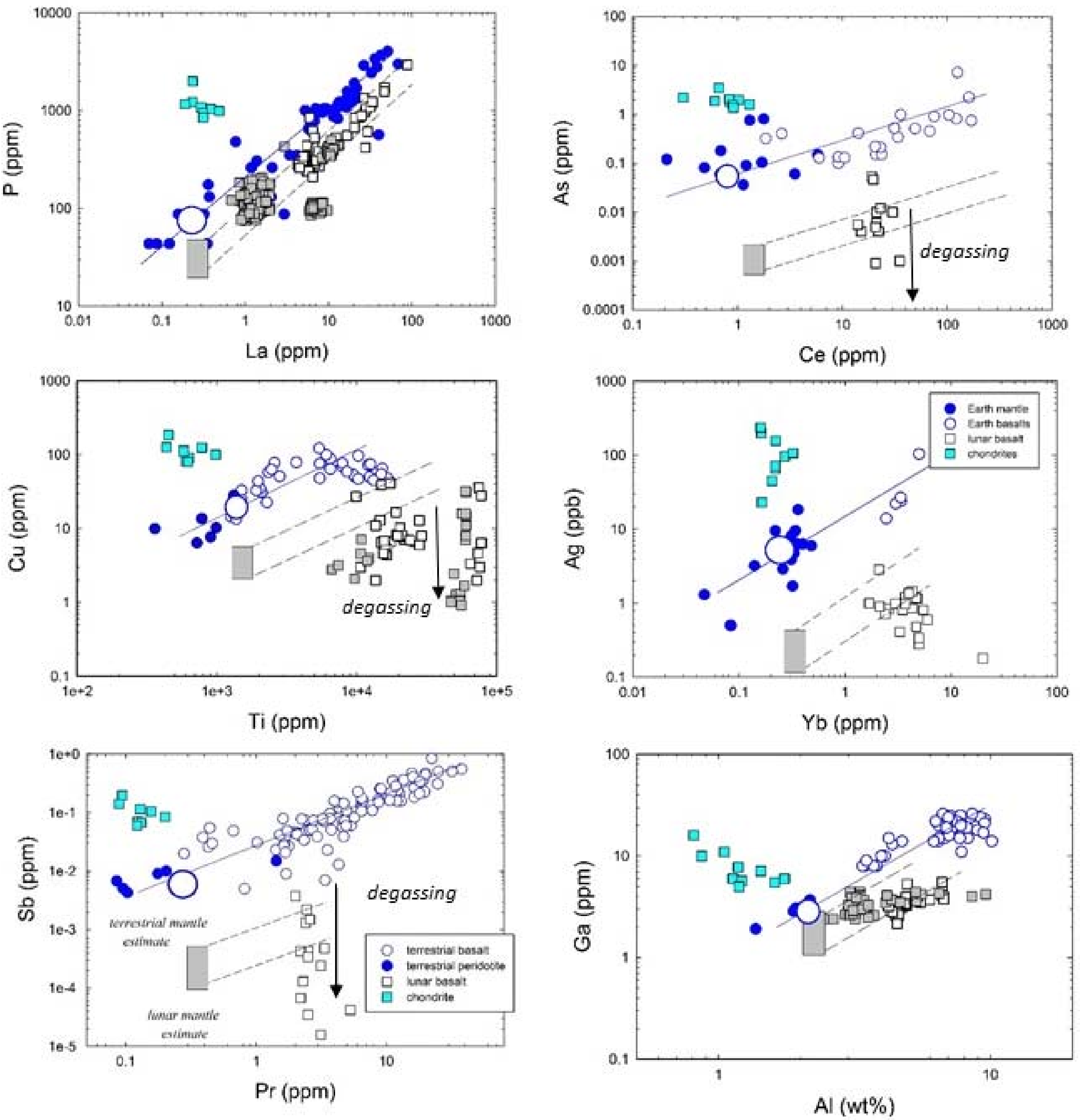
P (ppm)
La (ppm)
10000
1000
100
10
0.01
0.1
1
10
100
1000
As (ppm)
Ce (ppm)
100
10
1
0.1
0.01
0.001
0.0001
degassing
Cu (ppm)
Ti (ppm)
1e+2
1e+3
1e+4
1e+5
degassing
Ag (ppb)
Yb (ppm)
Earth mantle
Earth basalts
lunar basalt
chondrites
Sb (ppm)
Pr (ppm)
1e+0
1e-1
1e-2
1e-3
1e-4
1e-5
terrestrial mantle estimate
lunar mantle estimate
degassing
terrestrial basalt
terrestrial peridotite
lunar basalt
chondrite
Ga (ppm)
Al (wt%)

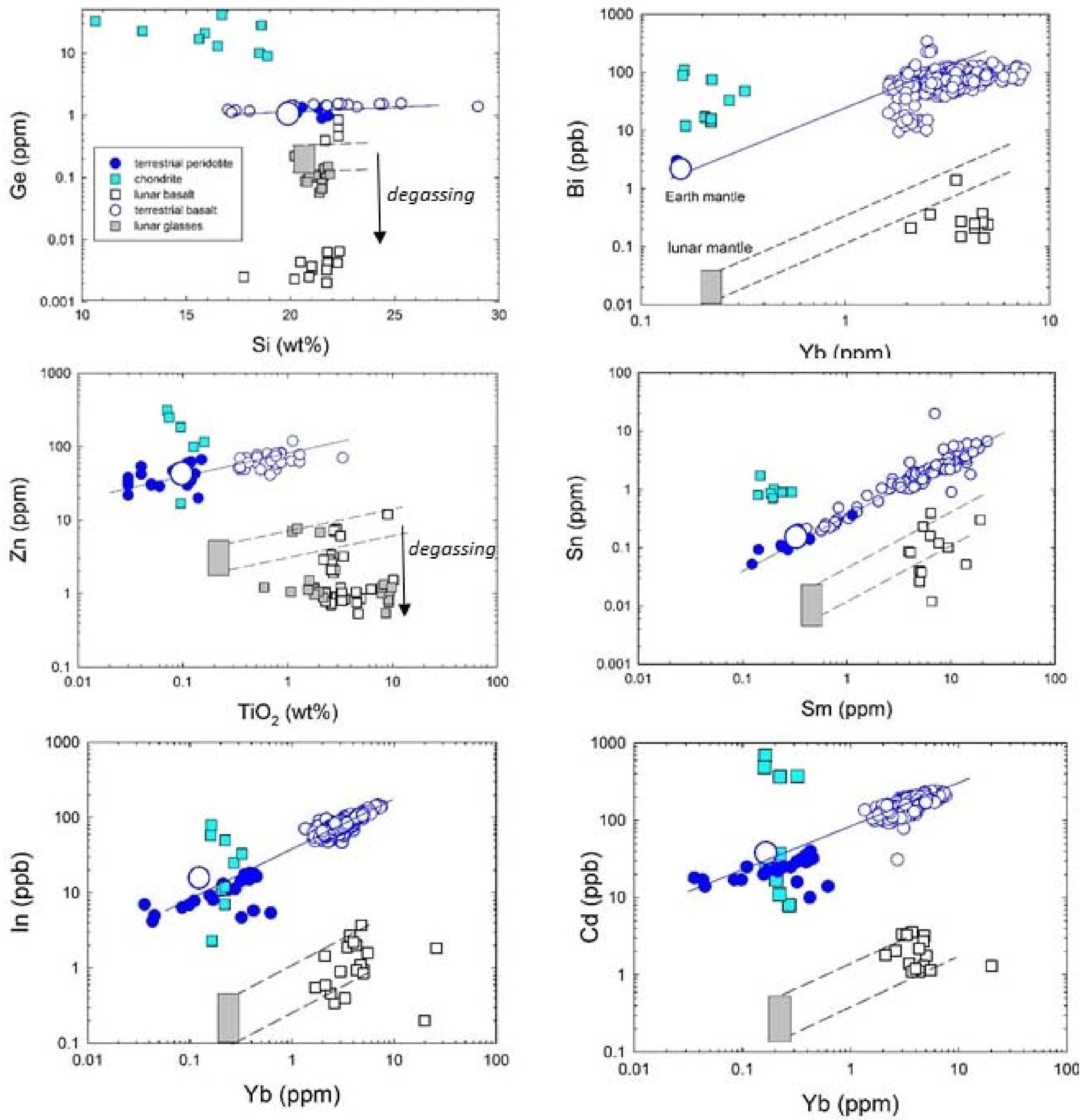

**Figure S2A:** Correlations of 12 VSE with a refractory lithophile element of similar degree of incompatibility. Solid blue lines highlight correlations in terrestrial peridotite (small closed circles) and basalt (small open circles) suites which are used as a guide for the lunar correlations. Cyan squares are chondritic data from the compilation of (88). Large open blue circles are the primitive mantle estimate from (37). The shaded gray box is the estimated range for the lunar mantle, at the corresponding mantle concentration of RLE (La, Ce, Ti, Yb, Pr, Al, Si, or Sm). Lunar basalts are open squares and lunar glasses are gray squares. A detailed discussion of the datasets and interpretation for each element is given in the accompanying supplementary text.

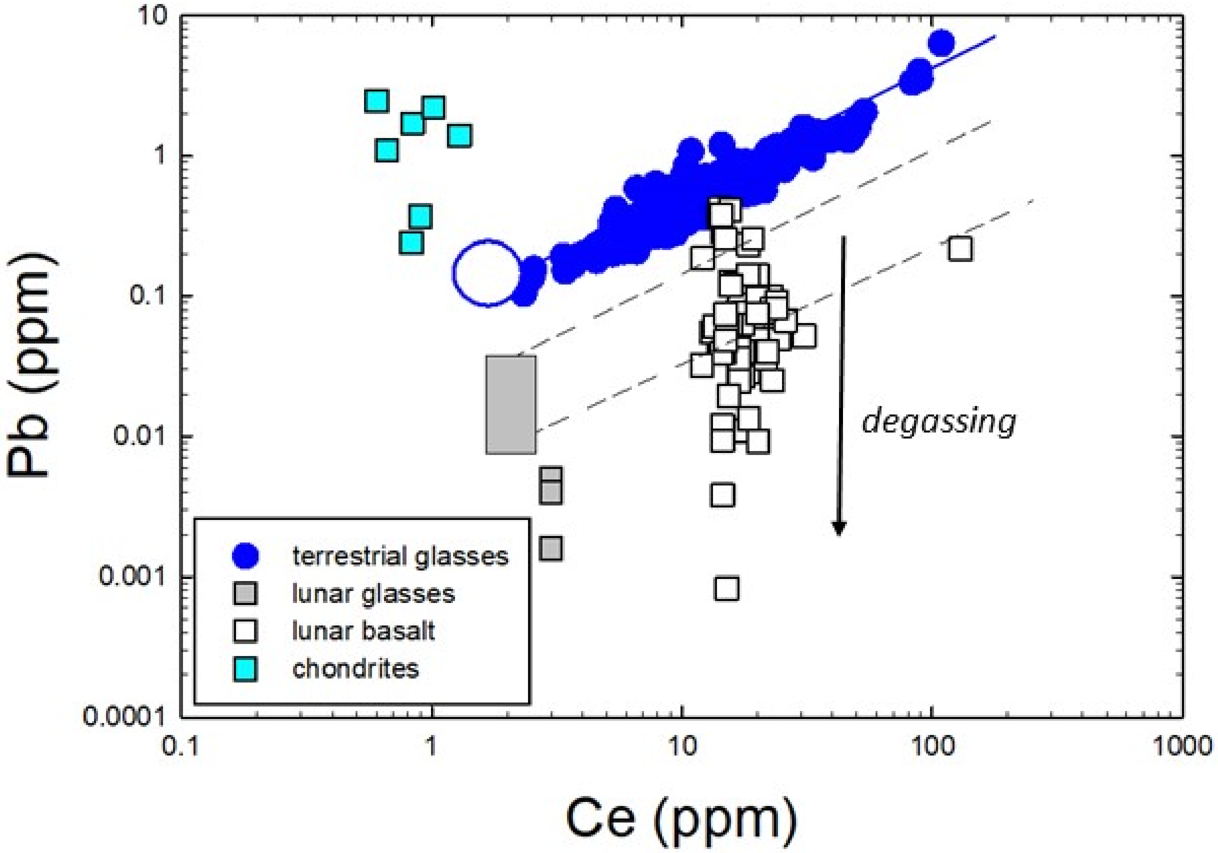

**Figure S2B:** Pb-Ce correlation showing depletion of Pb in lunar mantle compared to that in the terrestrial mantle. Lunar basalts are from (66, 89-94), Apollo 15 lunar glasses are from (91), while terrestrial glasses are from (95). The terrestrial mantle value is from (37). The lunar glasses fall well below the mare basalt samples, consistent with Pb loss due to magmatic volatility, and illustrate why Pb concentrations from glasses should not be used to derive lunar mantle Pb content. Pb concentrations are corrected for $^{206}$Pb, $^{207}$Pb, and $^{208}$Pb derived from decay of $^{232}$Th, $^{235}$U, and $^{238}$U, as described in the text.

## Table S1: Summary of bulk and mantle compositions, volatility corrections, activity coefficients, and core-mantle regression coefficients

| | **P (ppm)** | **As (ppb)** | **Cu (ppm)** | **Ag (ppb)** | **Sb (ppb)** | **Ga (ppm)** | **Ge (ppm)** | **Bi (ppb)** | **Pb (ppm)** | **Zn (ppm)** | **Sn (ppb)** | **Cd (ppb)** | **In (ppb)** | **Tl (ppb)** |
|---|---|---|---|---|---|---|---|---|---|---|---|---|---|---|
| | | | | | | | | | | | | | | |
| Mantle Moon¥ | 30(10) | 1.0(9) | 3.0(1.5) | 0.3(2) | 0.25(15) | 1.0(0.5) | 0.2(15) | 0.020(15) | 0.06(2) | 3(2) | 6(4) | 0.30(15) | 1.0(8) | 0.03(1) |
| | | | | | | | | | | | | | | |
| Bulk Moon (as PUM)[1] | 90(13) | 68(20) | 20(5) | 6(3) | 5.4(2.2) | 4.4(0.2) | 1.2(0.2) | 3(1) | 0.185(50) | 53.5(2.7) | 140(42) | 35(7) | 18(4) | 4.1(1.0) |
| D(gas/melt) | 3 | 4 | 5 | 6 | 7 | 8 | 9 | 15 | 20 | 30 | 40 | 60 | 80 | 100 |
| Depletion factor (mix) | 1 | 2 | 3 | 4 | 4 | 4 | 4 | 4 | 4 | 4 | 4 | 4 | 4 | 4 |
| Mantle Moon calc - hybrid | 91(20) | 0.4(1) | 6.8(2.0) | 0.40(08) | 0.30(10) | 0.9(5) | 0.15(05) | 0.03(01) | 0.05(2) | 11(3) | 22(5) | 7.1(2.8) | 3.6(1.8) | 1.0(4) |
| | | | | | | | | | | | | | | |
| Bulk Moon (as PMM)[2] | 675(90) | 86(15) | 2.0(0.5) | 4.2(0.8) | 20(4) | 6.6(2.2) | 0.6(0.3) | 0.6(0.3) | 0.38(8) | 19(4) | 39(8) | 10(4) | 7(3) | 1.3(5) |
| D(gas/melt) | 40 | 45 | 50 | 55 | 60 | 65 | 70 | 75 | 80 | 85 | 90 | 95 | 98 | 100 |
| Depletion factor (mix) | 1 | 5 | 6 | 7 | 7 | 7 | 8 | 8 | 9 | 9 | 9 | 10 | 10 | 10 |
| | | | | | | | | | | | | | | |
| Bulk Moon (as MSI)[3] | 10(2) | 1.0(5) | 15(5) | 1.0(5) | 0.02(1) | 1.0(5) | 0.8(3) | 0.001(1) | 0.17(5) | 53.5(2.7) | 2.0(8) | 30(8) | 25(7) | 4.1(1.0) |
| D(gas/melt) | 0.1 | 1 | 3 | 5 | 8 | 12 | 20 | 30 | 50 | 80 | 120 | 200 | 300 | 400 |
| Depletion factor (mix) | 1 | 2 | 3 | 4 | 4 | 4 | 4 | 4 | 4 | 4 | 4 | 4 | 4 | 4 |
| | | | | | | | | | | | | | | |
| $T_c$50 § | 1229 | 1065 | 1037 | 996 | 979 | 968 | 883 | 746 | 727 | 726 | 704 | 652 | 536 | 531 |
| $\gamma$ | 1.07 | 0.0182 | 6.24 | 91.5 | 0.395 | 1.01 | 0.036 | 347 | 590 | 0.99 | 1.77 | 1.0 | 16.6 | - |
| a | -1.06(11) | -0.68(37) | -0.083(61) | -0.09(2) | -0.66(16) | -0.90(8) | -0.41(4) | -0.49(11) | -0.51(8) | -0.76(6) | -1.14(8) | -0.69(6) | -1.07(21) | - |
| b | -70621 (6500) | -18545 (5860) | -5290 (4600) | +2002 (245) | -1700 (1200) | -63068 (2500) | -24090 (2600) | -7173 (2000) | -36263 (5900) | -48650 (4500) | -76870 (4560) | -47400 (4500) | -75860 (15500) | - |
| c | 2039 (170) | -42 (122) | -346 (310) | +200 (30) | 2050 (1050) | 1024 (63) | 680 (80) | +1000 (150) | +331 (186) | 891 (90) | +1340 (295) | +850 (90) | 1336 (290) | - |
| d | -1.23 (19) | -0.24 (6) | -0.35 (24) | -0.58 (25) | -0.73 (1.33) | -1.13 (11) | -0.26 (11) | 0.12 (3) | +0.062 (03) | 0.16 (9) | -0.27 (16) | +0.09 (4) | 0.09 (43) | - |
| e | 17.23 (1.87) | 12.64 (2.38) | 7.93 (2.88) | 8.53 (1.53) | -4.15 (1.23) | 17.3 (1.2) | 5.92 (1.17) | 8.46 (2.42) | +15.13 (2.88) | 6.77 (1.40) | 20.6 (2.5) | 9.8 (1.4) | 20.7 (5.0) | - |
| n | 122 | 33 | 50 | 58 | 51 | 169 | 85 | 24 | 76 | 96 | 104 | 42 | 44 | - |
| $r^2$ | 0.82 | 0.85 | 0.88 | 0.86 | 0.63 | 0.77 | 0.84 | 0.81 | 0.78 | 0.81 | 0.84 | 0.87 | 0.75 | - |
| $2\sigma$ | 1.51 | 1.02 | 0.94 | 0.69 | 2.50 | 1.18 | 0.80 | 0.61 | 1.14 | 0.61 | 1.64 | 0.80 | 1.65 | - |
| Reference | 4 | 5 | 4 | 7 | 5 | 4 | 5 | 7 | 4 | 4 | 6 | 6 | 5 | 8 |

¥ - values derived from element correlation diagrams in Figures S2A and S2B; uncertainty is defined in the figure, and discussed in Supplementary Information, Part 1).

PUM = primitive upper mantle of Earth; PMM = primitive martian mantle; MSI = Mars-sized impactor.

1 - Bulk Moon composition = primitive upper mantle of (37)
2 - Bulk Moon composition = primitive martian mantle of (96)
3 - Bulk Moon composition = calculated mantle of Mars-sized impactor (see Supplementary Information, part 2).
4 – (97)
5 – (11)
6 – (10)
7 – (98)
8 - D(Tl)metal/silicate = 1 based on work of (99, 100).

§ - 50% condensation temperature from (14).

γ - the activity coefficient calculated for lunar core formation using model and references given by footnotes 4,5,6,7.

a through e are regression coefficients from the experimental partitioning studies of footnotes 4,5,6,7; parenthetical numbers are 1σ error on the regression coefficient; n is the number of experiments included in the regression; $r^2$ is the correlation coefficient for the regression; 2σ represents the 2σ error on the regression which is also what is plotted in Figure 1 for all calculated lunar mantle values. Full discussion of the regression analysis and statistics are presented in the individual studies (10,11,97,98).

## 2 – Bulk Moon compositions

Three lunar bulk compositions - representing possible end members for Moon formation – are considered here:

(1) bulk Moon is from the terrestrial primitive upper mantle (37) as suggested in some formation models for the Moon (2,4, 35-37). This model is discussed in detail in the main text.

(2) bulk Moon is from the mantle of a Mars-sized impactor for which we will use Mars as a proxy; the mantle and bulk composition of Mars are relatively well known from meteorite studies and geochemical constraints (39,40, 96). Although there is no particular reason to think the Moon is Mars-like in composition, this example is included to illustrate what the results would be for a real example of a Mars-sized body of known composition, and for a body that is less volatile-depleted than the PUM.

(3) bulk Moon is from the mantle of a Mars-sized impactor, for which is used a CI chondrite bulk composition with an Earth-like volatility correction (see below), and segregated a core at the correspondingly lower PT conditions of a Mars-sized body. Additional assumptions are that the Mars-sized body had a 30% mass core (consistent with higher FeO in lunar mantle), melted to a depth of ~40% (typical for Earth and Mars) corresponding to P-T-$fO_2$ conditions of 15 GPa, 2300 °C, and IW-2. The resulting mantle concentrations from this differentiated Mars-sized impactor are calculated according to the partitioning studies of (11) for Ge, As, and Sb, (10) for Cd and In, (97) for P, Cu, Ga, Zn, and Pb, and (98) for Bi and Ag (summarized in **Table S1**). This bulk composition is slightly more volatile-depleted than the PUM.

## 3 - Disk mixing assumptions

Depletion of volatile lithophile elements (VLE) in the bulk compositions is guided by comparisons with Earth's primitive upper mantle, where Moon/Earth ratios are ~ 1 for Li, and ~0.25 for Na, K, Rb and Cs. The VLE can be used to constrain volatile depletions associated with disk mixing. Since the VLE between 800 and 1000 K are depleted to the same level ~ 4x lower in the Moon, mixing between a volatile-poor inner disk and volatile-rich outer disk can constrain the volatile depletions. Bulk compositions of the Moon are thus adjusted for the disk mixing calculations to satisfy the VLE concentrations. For the PUM bulk composition (as well as the third, Mars-sized impactor scenario, which utilizes the same bulk composition), this varies from a factor of 1 for P to a factor of 4 for most other VSE (Table S1 and Figure S3). The relatively volatile-rich nature of Mars requires a larger correction to get the observed ~4X volatile lithophile element depletion in bulk Moon relative to the Earth, and so for the PMM bulk composition, this varies from a factor of 1 for P to a factor of ~10 for the most highly volatile VSE such as In and Tl (Table S1 and Figure S3).

*PUM (and MSI) bulk composition:* Li has Tc(50%) = 1150 K, and has very similar concentrations in the lunar and terrestrial mantles (~1.6 ppm; (37), for PUM; 7 to 10 ppm Li in lunar basalts and glasses that may represent partial melting of a mantle with ~ 1.5 to 2 ppm Li using data from (101), and partitioning data of (102), indicating no loss of Li due to volatility. Thus no correction is applied to P which has an even higher Tc(50%) of 1229 K. Na, K, Rb, and Cs, however, have Tc (50%) of 1001, 996, 800, and 799 K, respectively) and so Ag, Sb, Ga, Ge, Bi, Pb, Zn, Sn, Cd, In, and Tl are all corrected by a factor of 4 to be consistent with these alkali elements. As and Cu, having intermediate Tc (50%) to Li and Na, are corrected by a factor of 2 and 3, respectively.

*PMM bulk composition:* Li has Tc (50%) = 1150 K and has very similar concentrations in the lunar and terrestrial mantles (see preceding paragraph), indicating no loss of Li due to volatility. Thus no correction is applied to P which has an even higher Tc(50%) of 1229 K. Na, K, Rb, and Cs, however, have Tc (50%) of 1001, 996, 800, and 799 K, respectively, and so Ag, Sb, and Ga are corrected by a factor of 7, Ge and Bi, are corrected by a factor of 8, Pb, Zn, and Sn are corrected by a factor of 9, and Cd, In, and Tl are corrected by a factor of 10. As and Cu, having intermediate Tc (50%) to Li and Na, are corrected by a factor of 5 and 6, respectively.

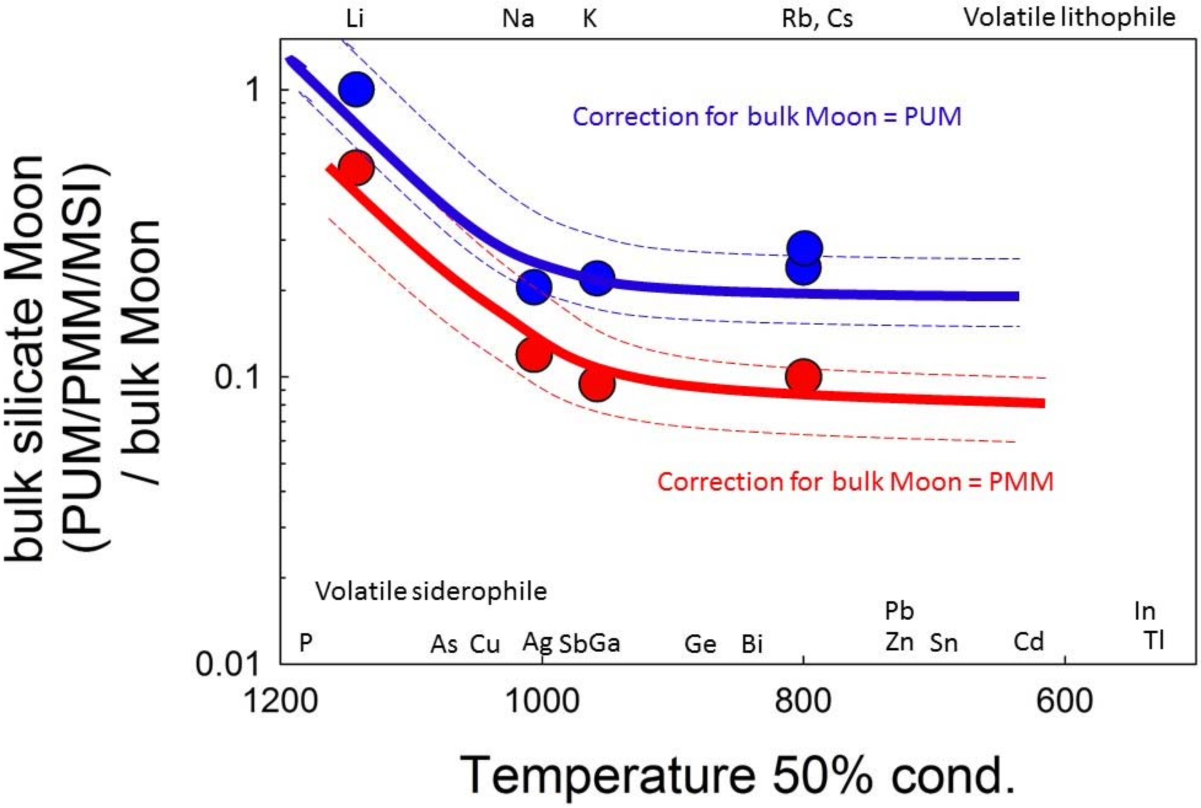

**Figure S3:** For disk mixing calculations, corrections are applied to VSE concentrations for the three bulk compositions considered here, based on volatile lithophile element (top axis: Li, Na, K, Rb, and Cs) concentrations in lunar samples and the terrestrial mantle. Blue symbols and line represent the correction applied to the bulk Moon = terrestrial PUM. Red symbols and line represent the correction applied to the bulk Moon = PMM (primitive martian mantle). Lines are estimates, not fit with any function, and the dashed lines are best estimate of uncertainty in the correction. There are no available volatile lithophile element data at temperatures <800 K. Values are normalized to the PUM, PMM, and MSI compositions. 50% condensation temperatures are from (14).

## 4 – Alternative models with impactor bulk compositions

Using the ***primitive martian mantle (PMM)*** composition for the bulk Moon, the two disk processes can be modelled as described in the text and supplementary material.

Modelling gas-melt equilibrium results in fits to P and Tl (as required by the gas-melt model, which uses D(P) gas-melt = 40 and D(Tl) gas/melt = 100, with a gas fraction of 0.5) as well as Bi and Cd, but most other elements are too low. After segregation of a small core, only As can be added to the list of elements that can be explained. Nine other VSE remain poorly fit in a scenario with gas-melt equilibrium using reasonable assumptions.

Modelling disk mixing results in fits to Ga, Pb, Zn, Sn, and In, but again most other elements provide a poor fit to the lunar mantle estimates. If disk mixing is combined with core formation, As, Ag, and perhaps Bi are improved, but there are still 6 elements of both moderately and highly volatile nature that are not fit well and in fact several orders of magnitude higher or lower than the lunar mantle estimates. Neither of these models – disk mixing or gas-melt equilibrium – work well for this bulk composition, and a hybrid model offers no help to elements such as Cu, Ge, or Sb that exhibit poor fits in the same direction for each model.

Hybrid models that consider both disk mixing and gas-melt equilibrium do not provide any improvements upon the two end members presented here. Therefore, modelling of this bulk composition does not lead to any viable solutions to the depletions of VSE in the Moon, as it is unclear what process would allow selected volatile elements to later be reconciled with the observed lunar mantle composition, without affecting the other VSEs.

Using the mantle of the Earth-like, but ***Mars-sized impactor (MSI)*** for the bulk Moon, the two disk processes can be modelled as described in the text and supplementary material.

Modelling gas-melt equilibrium results in fits to P and Tl (again, as required by the gas-melt model, which uses D(P) gas-melt = 0.1 and D(Tl) gas/melt = 400, with a gas fraction of 0.5) as well as As, Ag, and Cd, but most other elements are too low. After segregation of a small core, As does not fit anymore, and no additional elements are gained. Ten other VSE remain poorly fit in a scenario with gas-melt equilibrium using reasonable assumptions.

Modelling disk mixing results in fits to As, Cu, Ag, Ge, and Pb, but many VSE are too low such as Sb, Ga, Bi, and Sn, while Zn, Cd, In and Tl are too high. If disk mixing is combined with core formation, As and Ag no longer fit, and only Cu, Ge, and Pb do. There are still many elements of both moderately and highly volatile nature that are not fit well and in fact several orders of magnitude higher or lower than the lunar mantle estimates.

Neither of these models – disk mixing or gas-melt equilibrium – work well for this bulk composition, and a hybrid model offers no help to elements such as As, Sb, Ga, Bi, Sn, Cd, or Tl that exhibit poor fits in the same direction for each model. Therefore, modelling of this bulk composition does not lead to any viable solutions to the depletions of VSE in the Moon, as it is unclear what process would allow selected volatile elements to later be reconciled with the observed lunar mantle composition, without affecting the other VSEs.

In summary these two models where the bulk Moon is derived from the impactor, result in very different VSE concentrations than those estimated from sample suites.

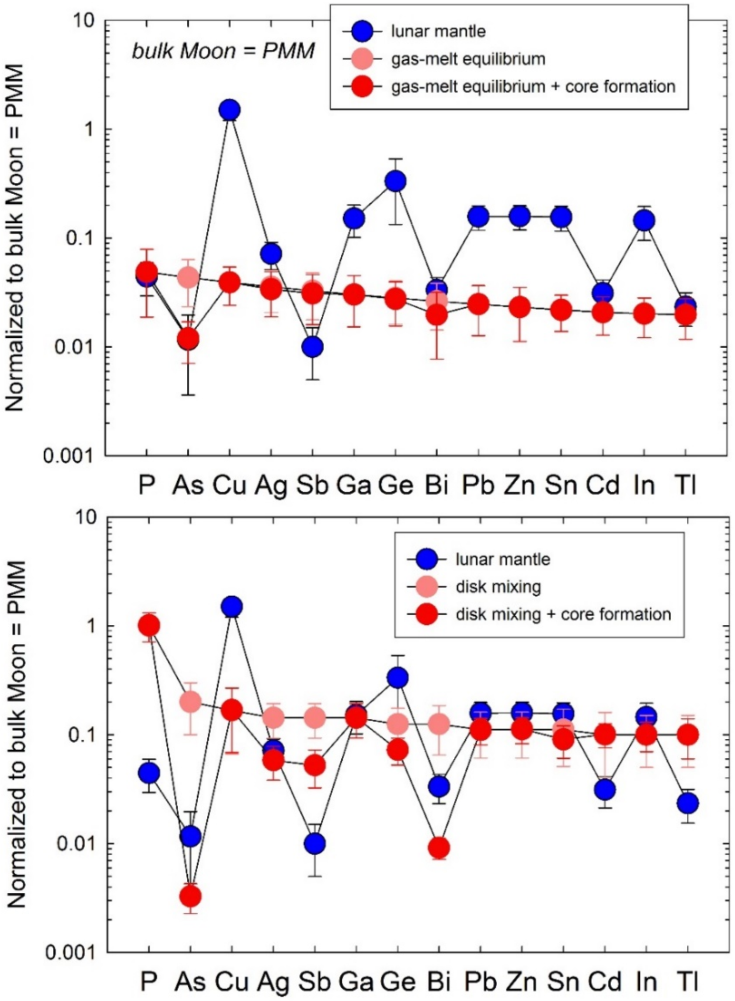

**Figure S4:** Fourteen volatile siderophile elements listed in the order of volatility as gauged by their 50% condensation temperature from (14). Blue symbols are lunar mantle estimates from correlations between the VSE and a refractory lithophile element (RLE) (see **Supplementary Information part 1** and **Figure S2**).

*Top:* Modelling gas-melt equilibrium (pink symbols) for bulk composition B (primitive martian mantle) results in fits to P and Tl (as required by the gas-melt model, which uses D(P) gas-melt = 40 and D(Tl) gas/melt = 100, with a gas fraction of 0.5) as well as Bi and Cd, but most other elements are too low. After segregation of a small core (red symbols), only As can be added to the list of elements that can be explained. 9 other VSE remain poorly fit in a scenario with gas-melt equilibrium using reasonable assumptions.

*Bottom:* Modelling disk mixing (pink symbols) for bulk composition B (primitive martian mantle) results in fits to Ga, Pb, Zn, Sn, and In, but again most other elements provide a poor fit to the lunar mantle estimates. If disk mixing is combined with core formation (red symbols), As, Ag, and perhaps Bi are improved, but there are still 6 elements of both moderately and highly volatile nature that are not fit well and in fact several orders of magnitude higher or lower than the lunar mantle estimates.

Neither of these models – disk mixing or gas-melt equilibrium – work well for a bulk composition of the primitive martian mantle.

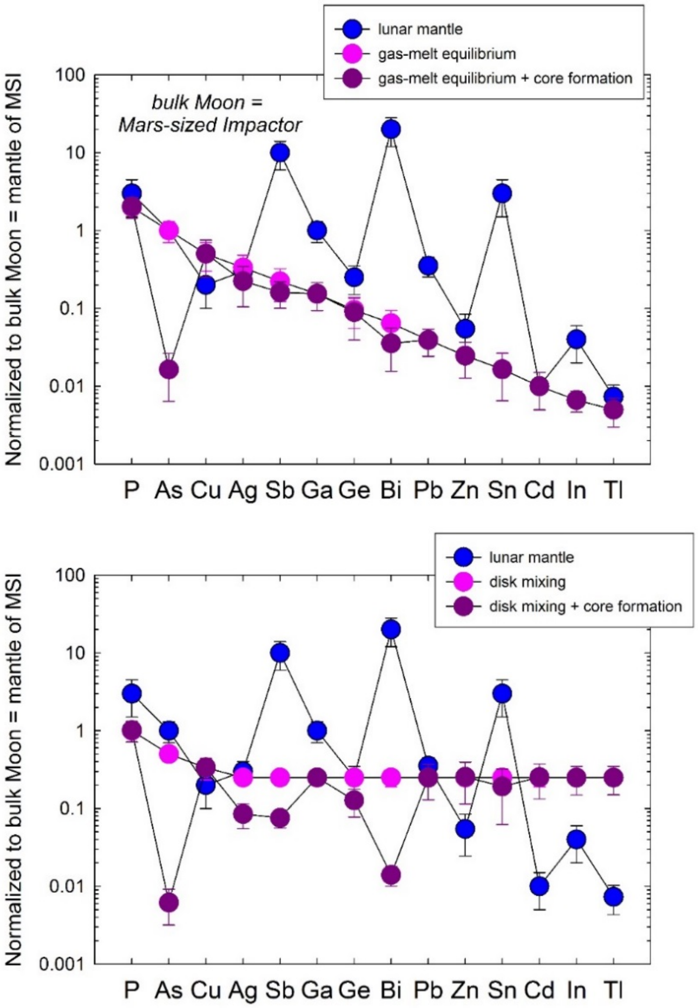

**Figure S5:** Fourteen volatile siderophile elements listed in the order of volatility as gauged by their 50% condensation temperature from (14). Blue symbols are lunar mantle estimates from correlations between the VSE and a refractory lithophile element (RLE) (see **Supplementary Information part 1** and **Figure S2**).

*Top:* Modelling gas-melt equilibrium (light purple symbols) for bulk composition C (Mars-sized impactor mantle) results in fits to P and Tl (again, as required by the gas-melt model, which uses D(P) gas-melt = 0.1 and D(Tl) gas/melt = 400, with a gas fraction of 0.5) as well as As, Ag, and Cd, but most other elements are too low. After segregation of a small core (darker purple symbols), As does not fit anymore, and no additional elements are gained. 10 other VSE remain poorly fit in a scenario with gas-melt equilibrium using reasonable assumptions.

*Bottom:* Modelling disk mixing (light purple symbols) for scenario C (Mars-sized impactor mantle) results in fits to As, Cu, Ag, Ge, and Pb, but many VSE are too low such as Sb, Ga, Bi, and Sn, while Zn, Cd, In and Tl are too high. If disk mixing is combined with core formation (darker purple symbols), As and Ag no longer fit, and only Cu, Ge, and Pb do. There are still many elements of both moderately and highly volatile nature that are not fit well and in fact several orders of magnitude higher or lower than the lunar mantle estimates.

Neither of these models – disk mixing or gas-melt equilibrium – work well for this bulk composition of a Mars-sized impactor mantle.